MOLECULAR BEAM STUDIES OF ELEMENTARY CHEMICAL PROCESSES

Nobel lecture, 8 December, 1986

by

YUAN TSEH LEE

Lawrence Berkeley Laboratory and Department of Chemistry, University of California, Berkeley, CA 94720, USA

Chemistry is the study of material transformations. Yet a knowledge of the rate, or time dependence, of chemical change is of critical importance for the successful synthesis of new materials and for the utilization of the energy generated by a reaction. During the past century it has become clear that all macroscopic chemical processes consist of many elementary chemical reactions that are themselves simply a series of encounters between atomic or molecular species. In order to understand the time dependence of chemical reactions, chemical kineticists have traditionally focused on sorting out all of the elementary chemical reactions involved in a macroscopic chemical process and determining their respective rates.

Our basic understanding of the relation between reactive molecular encounters and rates of reactions (formulated in terms of activation energies, E_a, and pre-exponential factors, A, as elucidated by Arrhenius in his rate constant expression, $k = A\exp(-E_a/kT)$), was deepened some fifty years ago following the discovery of quantum mechanics. Since a chemical reaction is fundamentally a mechanical event, involving the rearrangement of atoms and molecules during a collision, detailed information on the dynamics of simple chemical reactions could be obtained by first carrying our extensive quantum mechanical calculations of the interaction potential as a function of interatomic distances and then computing classical trajectories based on this potential energy surface [1]. Although these initial theoretical studies were only qualitative, they heralded a new era in the field of chemical kinetics; the chemist could now, in principle, predict the dynamical course of a chemical reaction.

During the past three decades, with the development of many sophisticated experimental techniques, it has become possible to study the dynamics of elementary chemical reactions in the laboratory. For example, detailed information on the nascent quantum state distributions of simple products for some chemical reactions can be derived from the chemiluminescence spectra of reaction products obtained under single collision conditions [2], the analysis of the threshold operating conditions of a chemical laser [3] or the spectra obtained using various linear or non-linear laser spectroscopic techniques [4, 5]. However, when one desires to (1) control the energies of the reagents, (2)

understand the dependence of chemical reactivity on molecular orientation, (3) explore the nature of reaction intermediates and their subsequent decay dynamics, and (4) identify complex reaction mechanisms involving polyatomic radical products, the crossed molecular beams technique is most suitable [6, 7].

Information derived from the measurements of angular and velocity distributions of reaction products played a crucial role in the advancement of our understanding of the dynamics of elementary chemical reactions. This and the more general investigations of chemical reactions under single collision conditions in crossed molecular beams will be the subject of this lecture.

Crossed Molecular Beams Experiments: Measurements of Angular and Velocity Distributions of Products.

If the motion of individual atoms were observable during reactive collisions between molecules, it would be possible to understand exactly how a chemical reaction takes place by just following the motion of these atoms. Unfortunately, despite recent advances in microscope technology that allow us to observe the static arrangement of atoms in a solid, we are still far from being able to follow the motion of atoms in the gas phase in real time. The idea of crossed molecular beams experiments is in a sense to "visualize" the details of a chemical reaction by tracing the trajectories of the reaction products. This is done by first defining the velocities, approach angle, and other initial conditions of the reactants, and then measuring the velocity and angular distribution of the products. For example, in the investigation of the $F + D_2 \rightarrow DF + D$ reaction [8], if we let F atoms and D_2 molecules collide at a relative energy of 1.82 kcal/mol and then measure the angular and velocity distributions of DF products, we will obtain the results shown in Fig. 1. This contour map shows the probability of DF products appearing at specific angles and velocities and reveals a great deal about the dynamics of the reaction. 0° corresponds to the initial direction of the F atom beam and the distance between any point and the center is the center-of-mass velocity. The strong backward peaking of DF products with respect to the initial direction of F atoms indicates that not all the collisions between F atoms and D_2 molecules produce DF product. Only those collisions in which the F atom and the two D atoms are nearly linear will react and produce DF. Apparently, if an F atom collides with a D_2 molecule from a direction perpendicular to the molecular axis of the D_2, the F atom will only bounce off elastically. The appearance of DF in several velocity bands is due to the fact that DF molecules are produced in several vibrational states with different recoil velocities as indicated in the figure. Since the total energy released in every reactive encounter between F and D_2 is the same, the maximum energy available for translational motion will depend on the vibrational quantum state of DF. Because the rotational energy spread of DF products is less than the spacings of the vibrational energy levels, the recoil velocities of various vibrational states of DF products are well separated and can be identified easily.

If a crossed molecular beams study of the $F + D_2 \rightarrow DF + D$ reaction is carried out using the an experimental arrangement shown in Fig. 2, the rate of
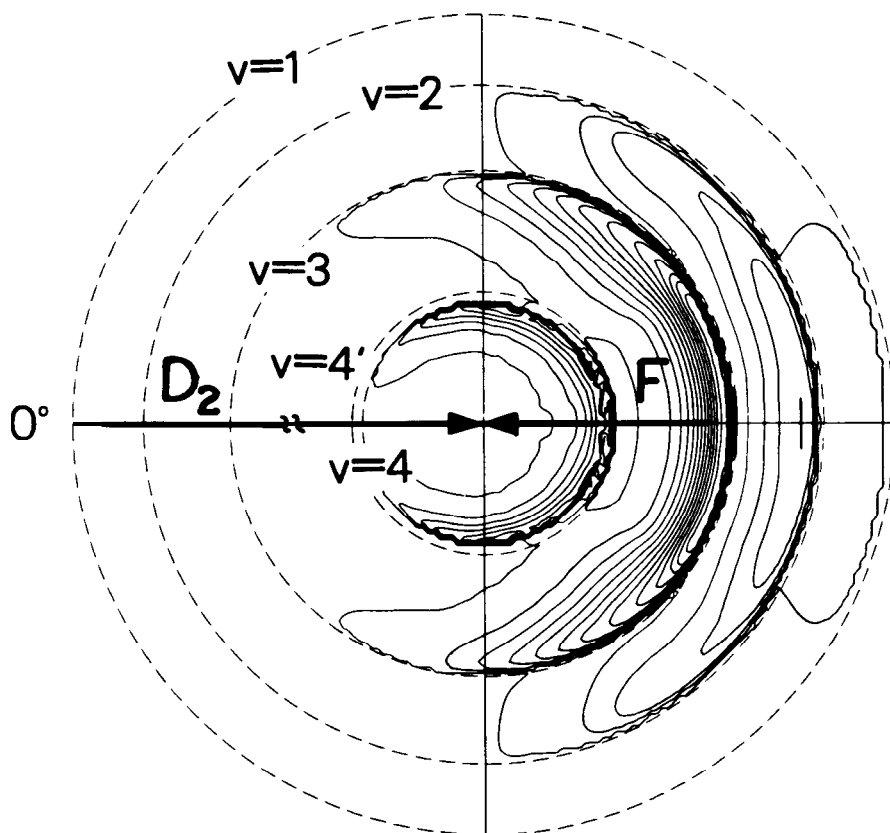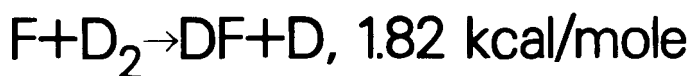
F+D$_2$→DF+D, 1.82 kcal/mole

Fig. 1. Center-of-mass velocity flux contour map for the F + D$_2$ → DF + D reaction. F atoms and D$_2$ molecules move towards each other at a collision energy of 1.82 kcal/mol, with the F atoms moving from right to left.

production of DF products, dN$_{DF}$/dt, in the scattering volume defined by the crossing of two beams can be estimated from the following equation:

$$\frac{dN_{DF}}{dt} = n_F n_{D2} \sigma g \Delta V$$

where n$_f$ and n$_{D2}$ are the number densities of F atoms and D$_2$ molecules in the scattering region, σ, g, and AV are the reaction cross section, the relative velocity between F and D$_2$ and the scattering volume, respectively. In a experiment using a velocity selected effusive F atom source and a supersonic beam of D$_2$, the values of n$_F$, n$_{D2}$, and AV are typically 10^{10} molecules/cc, 10^{12} molecules/cc, and 10^{-2} cc. If the relative velocity between F and D$_2$ is 10^5 cm/sec and the reactive cross section is 10^{-15} cm^2, the dN$_{HF}$/dt will have a value of
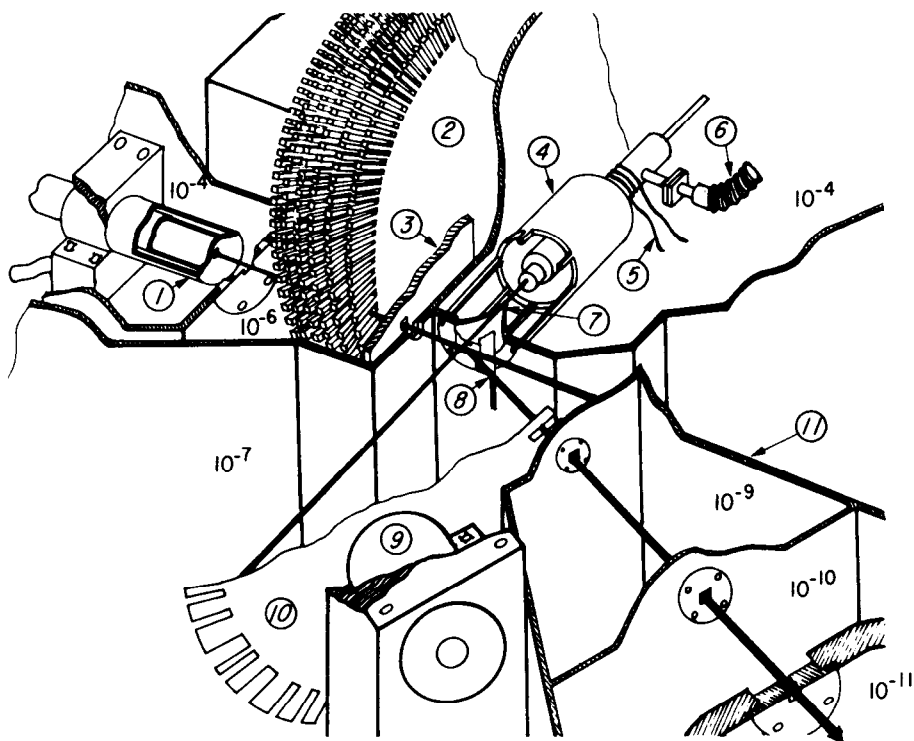
Fig.2. Experimental arrangement for F + $D_2 \rightarrow$ DF + D and F + $H_2 \rightarrow$ HF + H reactive scattering. Pressures (in torr) for each region are indicated. Components shown by numbers are: (1) effusive F atom beam source made of nickel, resistively heated; (2) velocity selector; (3) liquid nitrogen cooled cold trap; (4) D_2 or H_2 beam source, supersonic expansion, (5) heater, (6) liquid nitrogen feed line, (7) skimmer, (8) tuning fork chopper, (9) synchoronous motor, (10) cross correlation chopper for time-of-flight velocity analysis, (11) ultrahigh vacuum, triply differentially pumped, mass spectrometric detector chamber.

10^{10} molecules/sec. These DF products with various recoil velocities will scatter into a range of laboratory angles. If the DF is scattered fairly evenly within 1 steradian of solid angle in the laboratory and if the movable detector which scans the angular distribution has an acceptance solid angle of 1/3000 steradian (approximately an angular width of 1° in both directions from the detector axis), the detector will receive ~3 $\times$ 10^6 DF molecules per second.

This would certainly constitute a large product signal, assuming we were able to count all of these molecules. Indeed, in a reactive scattering experiment using a beam of alkali atoms, surface ionization could be used to detect the alkali containing product with nearly 100 percent efficiency and with high specificity. Therefore, even in the presence of a billion times more background molecules very good signal to noise ratios can be obtained in a short time.

To detect the DF products, however, first it is necessary to ionize DF to DF$^+$ by electron bombardment. The product ion can then be mass filtered and counted. The typical ionization efficiency for a molecule during the short transit time through the ionizer is about 10^{-4}. 3 x 10^6 DF/sec reaching the

detector will yield only 300 DF[+] ions/sec. However, this is a large enough
number to allow reliable measurements of angular and velocity distributions in
a relatively short time if the background count rate is not much greater.
Indeed, the success of a crossed molecular beams study of such a chemical
reaction depends entirely on whether the background in the mass spectrometric
detector can be reduced sufficiently [9].

There are two sources of background molecules in the detector that one has
to deal with in a crossed molecular beams experiment: the inherent background
in the detector chamber and the background caused by the effusion of mole-
cules from the collision chamber into the detector when the beams are on. The
former is mainly due to outgassing from the materials used for the construction
of the chamber and to limitations imposed by the performance of the ultrahigh
vacuum pumping equipment. Reduction of the latter requires many stages of
differential pumping using buffer chamber. 3×10^6 molecules/sec entering the
detector with a speed of 10^5 cm/sec through a 0.3 cm^2 aperture will establish a
steady state density of only 100 molecules/cc, which is equivalent to a DF
pressure of about 3×10^{-15} torr. This is four orders of magnitude lower than
the pressure attainable using conventional ultrahigh vacuum techniques. Since
none of the chemical compounds found in a vacuum system give ions with a
mass-to-charge ratio (m/e) of 21 (DF[+]) in the ionization process, inherent
background will not be a problem for the investigation of the $F + D_2 \rightarrow DF + D$
reaction even if the ultimate pressure of the detector chamber is around 10^{-11}
torr.

Suppose the partial pressure of DF background molecules in the collision
chamber after the introduction of beams of F atoms and D_2 molecules reaches
$\sim 10^{-9}$ torr. Then three stages of differential pumping will be required to obtain
a partial pressure of $\sim 10^{-15}$ in the ionizer chamber if the partial pressure of DF
is reduced by a factor of 100 in each separately pumped buffer chamber. As
long as the inherent background in the detector does not contain the species to
be detected, extensive differential pumping appears to be the only thing needed
to make reactive scattering experiments feasible. This conclusion is unfortunate-
ly not quite correct. In order to detect the scattered products, the defining
apertures, which are located on the walls of the buffer chambers of the detector,
must be perfectly aligned. This limits the reduction of background that would
be possible through many stages of differential pumping since some of the DF
molecules in the main chamber moving along the axis of the detector will pass
straight through all the defining apertures and into the detector chamber. It is
important to understand that no matter how many stages of differential pump-
ing are arranged between the collision chamber and the detector chamber, the
number of these "straight through" molecules can not be reduced.

If all the apertures on the walls of the buffer chambers and the detector
chamber have the same area, A, the steady state density of "straight through"
molecules in the detector chamber, n', at a distance d from the entrance
aperture of the first buffer chamber can be calculated from the following
relation

$$n' = \frac{nA}{4\pi d^2}$$

where n is the number density of background molecules in the collision chamber. If d is 20 cm and A is 0.3 cm^2

$$n' = \frac{0.3}{4\pi \cdot (20)^2}\, n \approx 6 \times 10^{-5} n.$$

If the partial pressure of DF background molecules in the collision chamber is 10^9 torr, the "straight through" molecules will create a steady state density of 6×10^{-14} torr, which is 60 times larger than what one hopes to accomplish with 3 stages of differential pumping. Of course, reduction of the partial pressure of DF molecules in the collision chamber will also reduce the "straight through" background, but increasing the pumping speed in the collision chamber to reduce the partial pressure of DF by several orders of magnitude is simply not a practical solution.

Fortunately there is a way to reduce this background without substantially increasing the pumping speed in the collision chamber. Recognizing that at a pressure of 10^{-7} torr the mean free path between molecular collisions in the collision chamber is more than 100 meters, which is two orders of magnitude larger than the size of a typical scattering apparatus, one realizes that almost all of the "straight through" background will come from those molecules that bounce off the surface which is in the line-of-sight of the detector, and not from gas phase collisions that occur in the viewing window of the detector. Installing a small liquid helium cooled surface opposite the detector and behind the collision region, such that the detector line-of-sight always faces a cold surface, will help to eliminate this background since the surface will trap essentially all condensable molecules that impinge on it.

Since the mid-1960's, many "universal" crossed molecular beams apparati have been constructed in various laboratories. Since ultrahigh vacuum equipment available twenty years ago could attain an ultimate pressure of only $\sim 10^{-10}$ torr, and only two stages of differential pumping were needed to reduce the pressure from 10^{-7} torr in the collision chamber to 10^{-10} torr in the detector chamber, almost all mass spectrometric detectors with electron impact ionization were constructed with no more than two stages of differential pumping, the principal exceptions being those built in our laboratory [10]. The failure to recognize that for many chemical species the partial pressure in the detector chamber could be reduced well below the ultimate total pressure through additional differential pumping was part of the reason why many of these apparatuses did not perform optimally.

Direct Experimental Probing of Potential Energy Surfaces
For gaseous rare gas systems, if the interaction potentials between the atoms are accurately known, all bulk properties and transport phenomena can be predicted theoretically. Similarly, for a simple atom-molecule reaction, the potential energy surface, which describes the interaction potential as a function

of the coordinates of the atoms, will be the basis for the understanding of the detailed dynamics of a chemical reaction.

One of the systems which has attracted extensive attention in both experimental and theoretical efforts during the last fifteen years is the reaction of $F+H_2 \rightarrow HF+H.$ In the early 1970's, using quasi-classical trajectory calculations, Muckerman derived a semiempirical potential energy surface, known as the Muckerman V surface, which gave results in agreement with all experimental data available at that time [11]. These results included rate constants, vibrational-rotational state distributions obtained from chemical laser and chemiluminescence experiments, as well as product angular distributions obtained from $F+D_2 \rightarrow DF+D$ experiments as shown in Fig. 1. The potential energy surface obtained from the ab initio quantum mechanical calculations [12] was still rather limited at that time, but it did show many important features which were in good qualitative agreement with the Muckerman V surface.

If the Muckerman V surface were sufficiently accurate, it would be possible to carry out scattering calculations using this surface under conditions which could not be easily arranged in the laboratory. This would significantly expand the scope of our understanding of the dynamics of this system. However, the accuracy of the Muckerman V surface depends not only on the reliability of the experimental input used in the derivation of the surface, but also on the applicability of classical mechanics in treating the $F+H_2 \rightarrow HF+H$ reaction. This is certainly a major concern for a H atom transfer reaction.

One dimensional quantum calculations on the $F+H_2$ reaction, although not necessarily realistic, had in fact shown the inadequacy of classical mechanics in handling this reaction [13, 14]. Quantum effects were, indeed, very important, and in all these calculations strong "resonances" were found in the dependence of reaction probability on collision energy [15]. These resonances were later shown to be due to the formation of "quasi-bound" states in the F-H-H reaction intermediate [16, 17]. The $F+H_2$ surface has a barrier in the entrance channel, but there is no attractive well in the intimate region near the transition state. The quasi-bound states in the $F+H_2$ reaction are entirely dynamical in nature. Loosely speaking, the first dynamic resonance is due to the formation of a bound state which is a superposition of $F+H_2$ (v = 0) and HF (v=3)+H in the intimate region of chemical interaction.

The discovery of dynamical resonances in the collinear quantal calculations of the $F+H_2$ system provided new possibilities for probing the critical region of the potential energy surface more directly. In contrast to most other microscopic experiments, in which the influence of the potential energy surface on the final distribution of products is assessed, the experimental observation of resonances is almost equivalent to carrying out vibrational spectroscopy directly on the reaction intermediate. Thus it should offer a more stringent test of the details of the calculated potential energy surface [16].

In a three dimensional quantum scattering calculation of $F + H_2$ on the Muckerman V surface, Wyatt et al. [18] have shown that as the collision energy is increased beyond the one dimensional resonance energy, the reso-
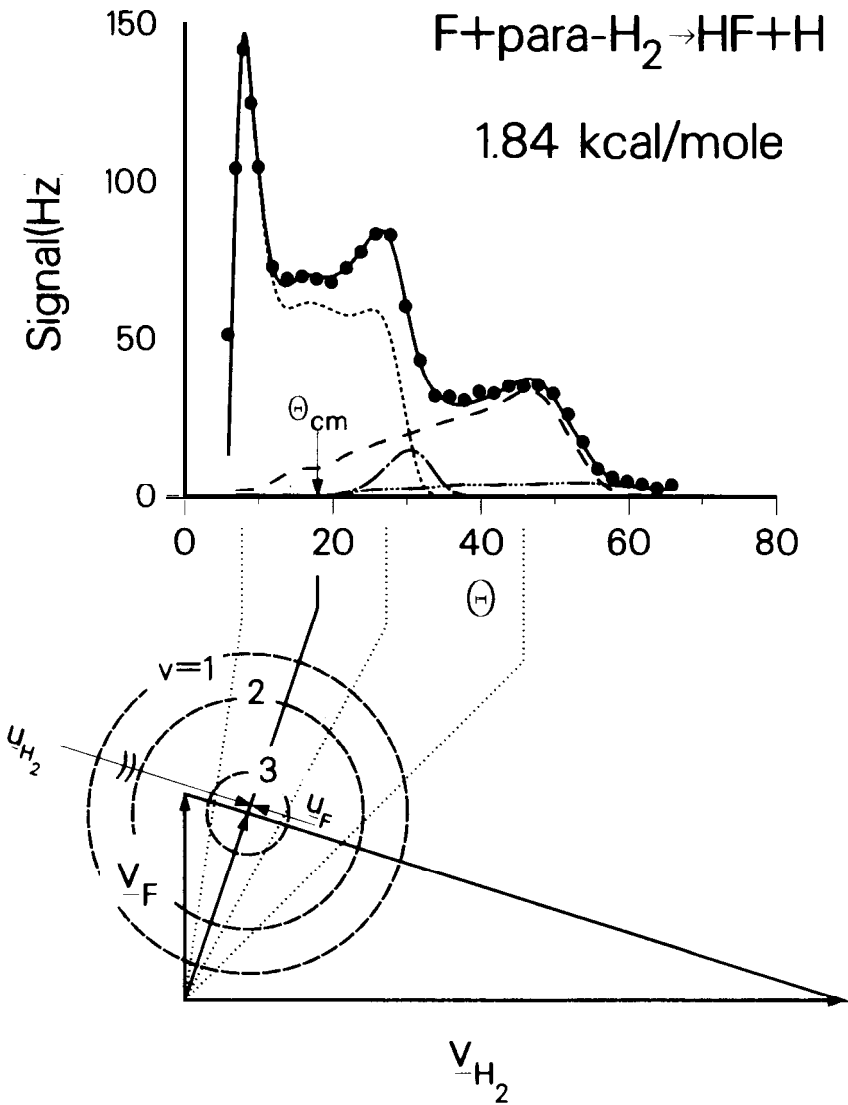
Fig 3. Laboratory angular distribution for F + para-H₂, 1.84 kcal/mol, velocity diagram shown below. Both the data and calculated laboratory distributions are shown (● data, ----- total calculated, — · · · — v=1, - - - v=2, · · · · · · v=3 — · — v=3, (from H₂(J=2)).

nance does not just disappear but occurs at increasingly larger impact parameters. Consequently, resonances cannot be observed in an experiment in which the reaction cross section is measured as a function of collision energy. On the other hand, if the experiment is carried out at a fixed collision energy, and if the reaction probability is measured as a function of impact parameter, the resonance should be observable. Unfortunately, one has no hope of controlling or
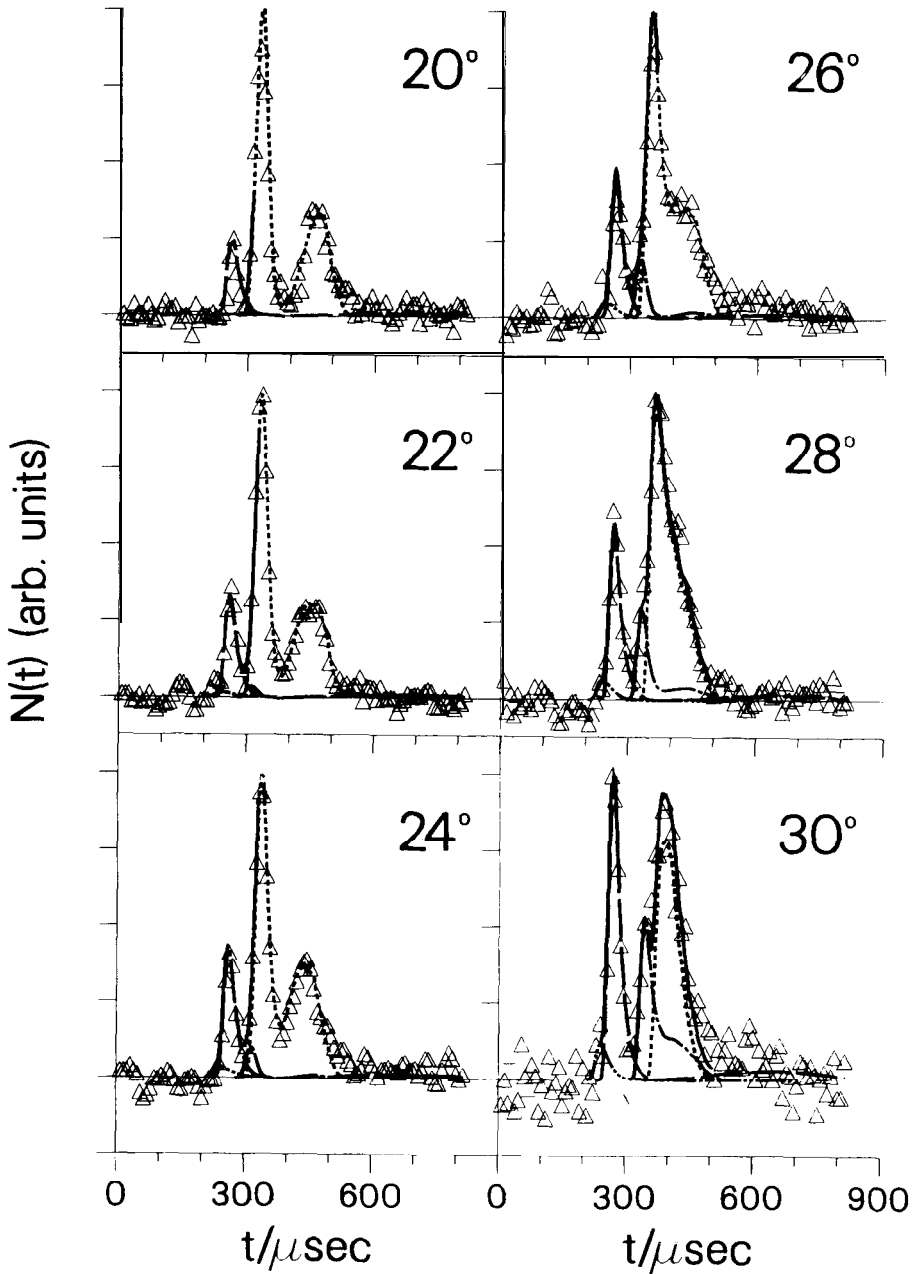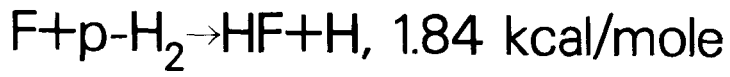
F+p-H$_2$→HF+H, 1.84 kcal/mole
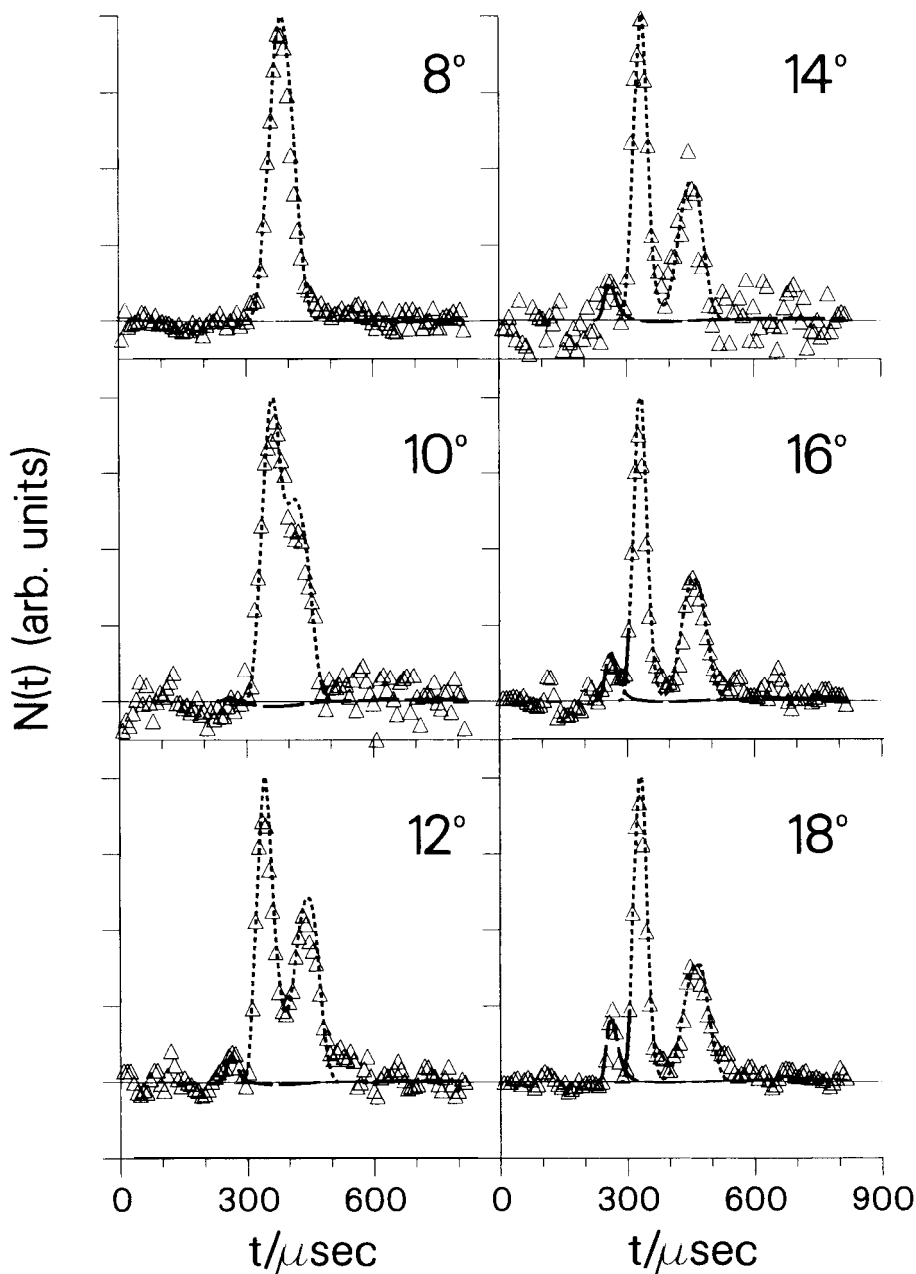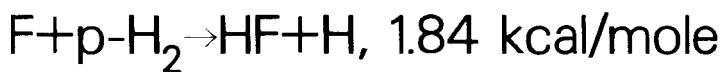
Fig. 4(a). Time-of-flight spectra for F + para-H$_2$, 1.84 kcal/mol. (△ data, ———total calculated, ——···— v=1, – – – v=2, - - - - - v=3, —·— v=3′.

F+p-H₂→HF+H, 1.84 kcal/mole

XBL 841-38

Fig. 4(b)

$F+p-H_2 \rightarrow HF+H$, 1.84 kcal/mole
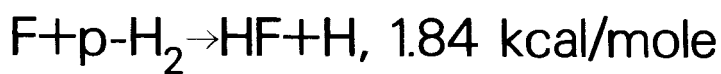
Fig. 4(c)
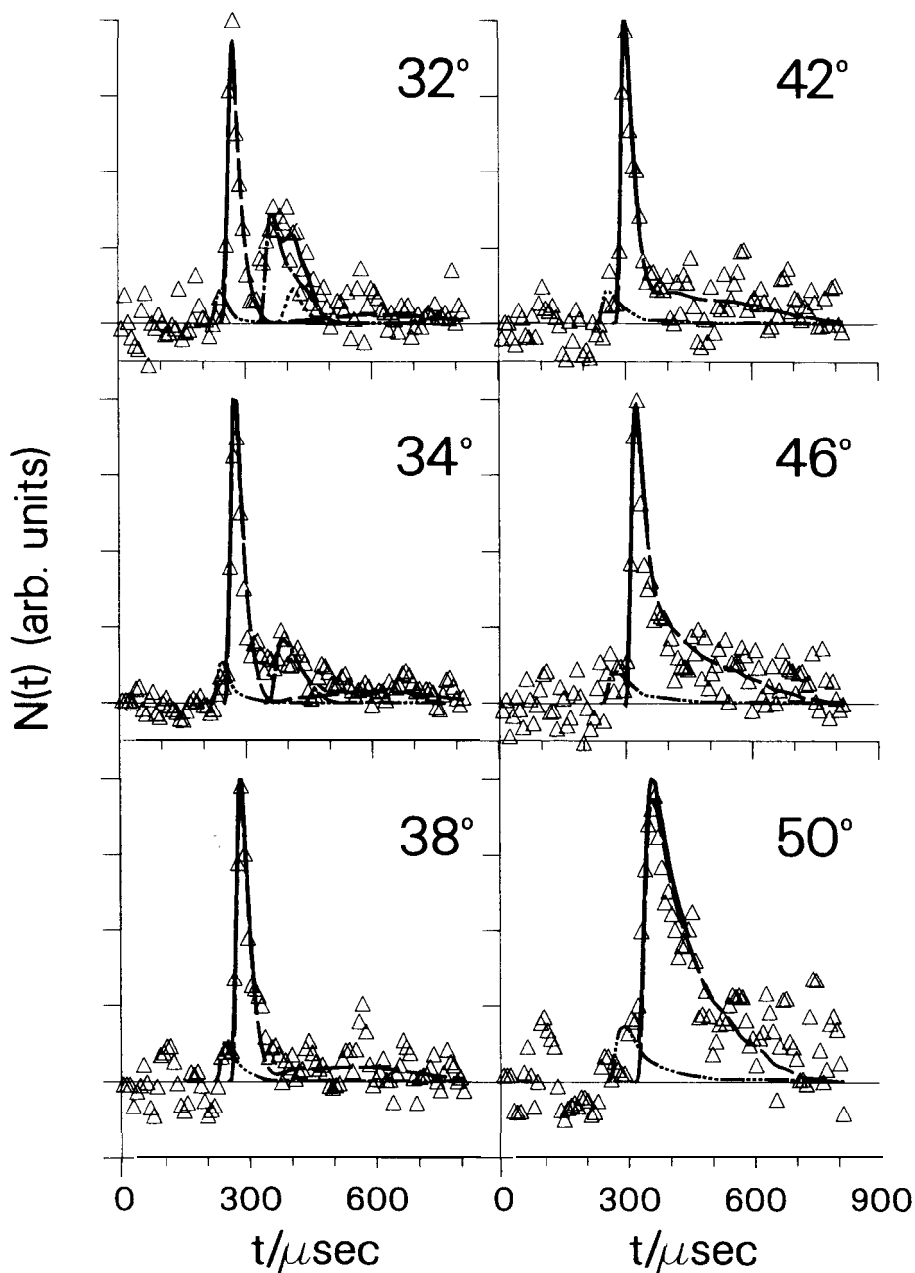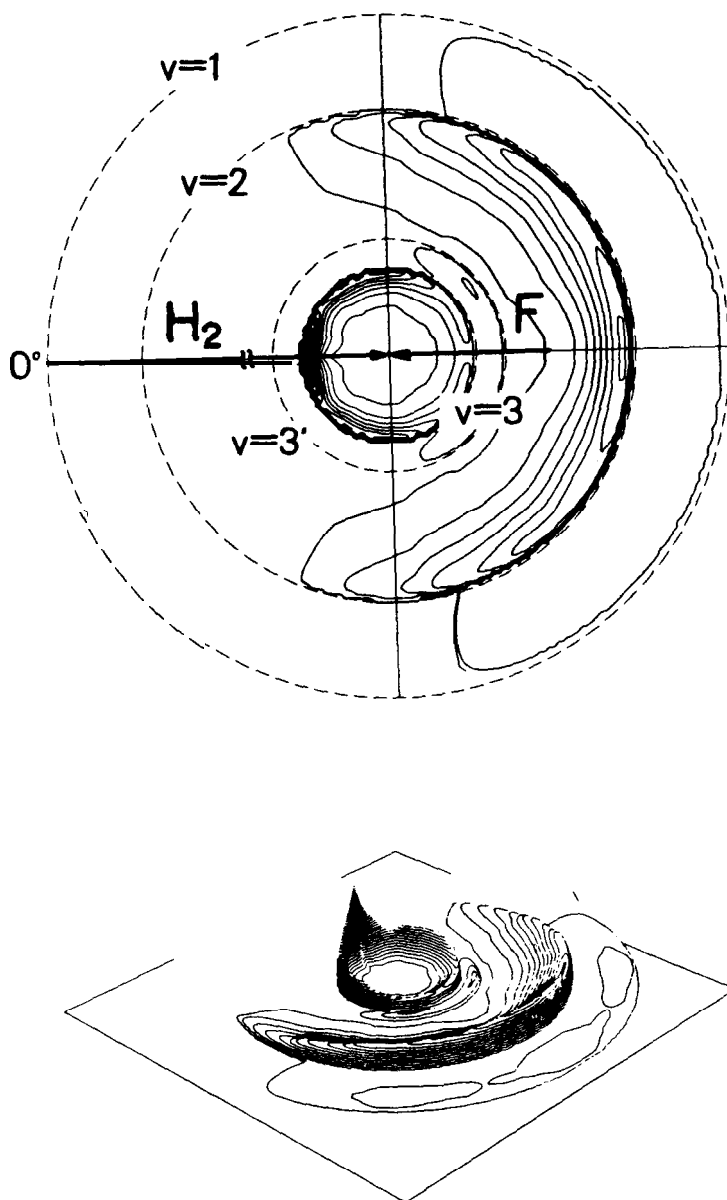
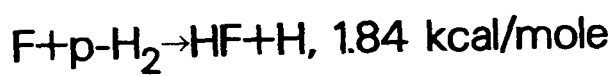XBL 841-39

F+p-H₂→HF+H, 1.84 kcal/mole

Fig. 5. Center-of-mass velocity flux contour map for F + para-H₂, 1.84 kcal/mol, shown in three dimensional perspective.

measuring the impact parameter in a scattering experiment. But, for F + H$_2\rightarrow$ HF + H, in which the collinear configuration dominates the reactive scattering at lower collision energies, the scattering angle of HF should depend on the impact parameter. In particular, when a quasi-bound state is formed, if the average lifetime of the F-H-H intermediate is an appreciable fraction of its rotational period, HF produced from the decay of the F-H-H quasi-bound state is expected to scatter in a more forward direction compared to the strongly backward peaked HF produced by direct reaction. One of the unique and most important aspects of the measurement of product angular distributions is that one can use the rotational period of the reaction intermediate, typically 10^{-12}-- 10^{-13} sec to judge the lifetime of the reaction intermediate [6]. If the average lifetime of the intermediate is much longer than the rotational period, the angular distribution of products will show forward-backward symmetry. On the other hand, if the lifetime is much shorter, the asymmetric angular distribution reveals the preferred molecular orientation for the chemical reaction to occur.

Experimental measurements of the laboratory angular distribution and time-of-flight velocity distributions of HF products at a collision energy of 1.84 kcal/mole, using the experimental arrangement shown in Fig. 2, are shown in Figs. 3 and 4. The velocity and angular distributions in the center-of-mass coordinate system derived from these experimental results are shown in Fig. 5 [19]. The enhanced forward peaking in the angular distribution of HF in v=3 is a strong indication that quasi-bond states are indeed formed in the F + H$_2\rightarrow$ HF + H reaction at this energy, and that they seem to decay exclusively into HF in the v=3 state.

For the reaction of F + HD $\rightarrow$ HF + D, quantal collinear calculations give a very striking result. There is a sharp spike in the HF(v=2) reaction probability near threshold and virtually no other product is formed at higher collision energies up to 0.2 eV [15]. The collinear calculations therefore indicate that the formation of HF in this reaction is dominated by resonant scattering while the DF product is formed by direct scattering. As shown in Fig. 6, the product angular distribution of HF measured at a collision energy of 1.98 kcal/mol indeed shows that most of the signal is in the forward direction as expected, in strong contrast to the DF signal which is formed through direct scattering and is therefore mainly scattered in the backward direction. Again, the forward peaked HF products are found to be in the v=3 state, rather than v=2, as was observed in the quantal calculations on F + H$_2\rightarrow$ HF + F. This disagreement is certainly due to the shortcoming in the M5 surface. These vibrationally state specific angular distributions obtained at various collision energies for F + H$_2$, HD and D$_2$ reactions provide a very stringent test for the ever improving potential energy surfaces obtained from ab initio quantum mechanical calculations.

There is no doubt that through meaningful comparisons with experimental results, more sophisticated and reliable ab initio quantum mechanical calculation techniques will emerge. In the near future, ab initio calculations of potential energy surfaces and exact scattering calculations on these systems will
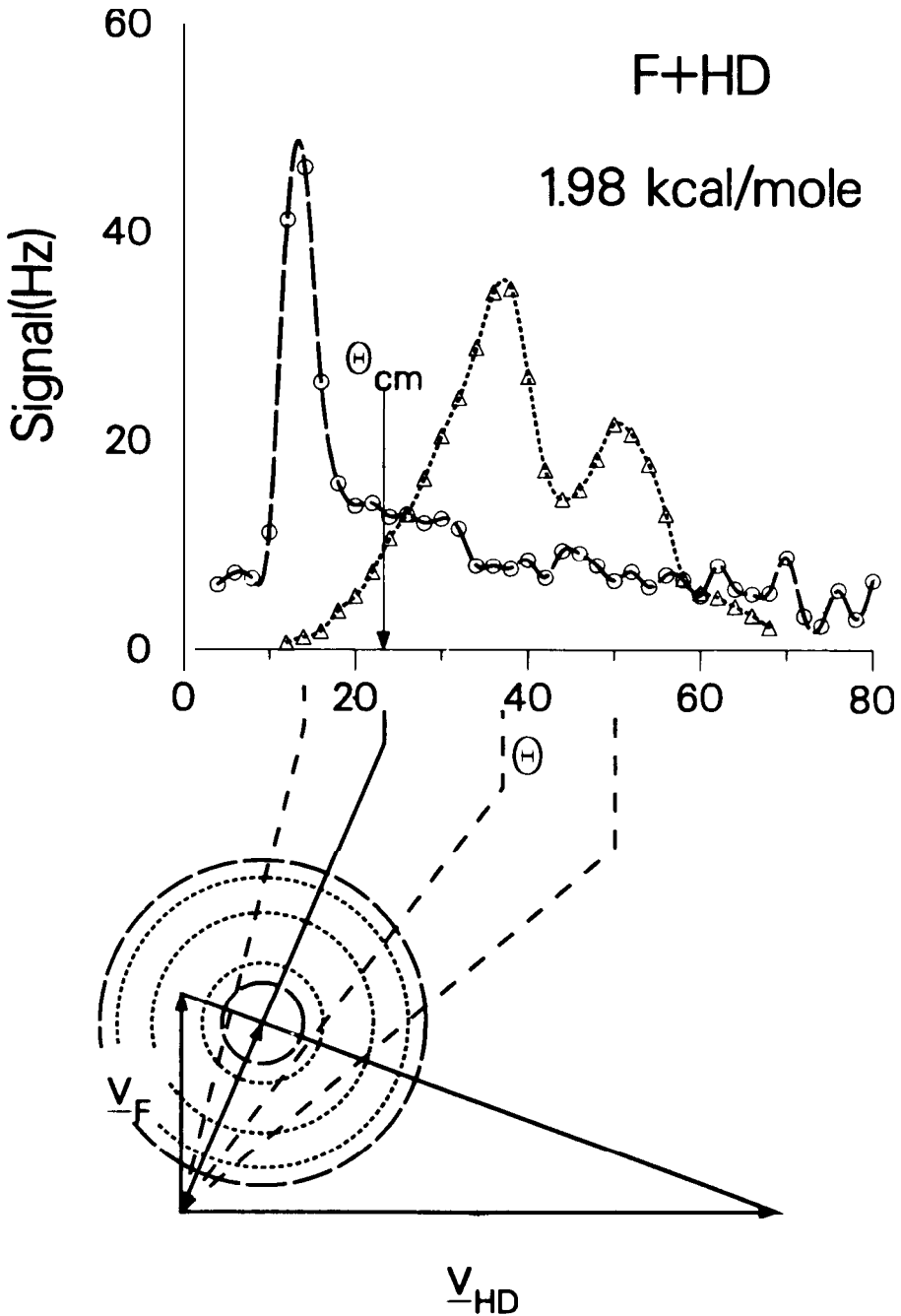
Fig. 6. Laboratory angular distribution for F + HD, at a collision energy of 1.98 kcal/mol (– – – ○ – – – ○ – – – HF product, ...△....△ ..... DF product). The Newton circles corresponding to HF and DF product are drawn with the same texture as the lines in the angular distributions. The HF (v=3) and v=2 circles are shown, as are the v=4, 3, and 2 circles for DF.

likely provide more detailed and accurate information in simple reactive systems such as F + H$_2$ than one could possibly learn in the laboratory. The fruitful interplay of theory and experiment will then extend to more complicated systems, making chemistry a more exact science.

Exploration of new chemistry under single collision conditions

There are many mysterious phenomena in nature which have thus far defied explanation. The mystery is often due to the fact that a certain phenomenon cannot be understood based on our established knowledge or common sense.

The ease with which F$_2$ and I$_2$ react to produce electronically excited IF molecules which relax through photon emission was a mystery a dozen years ago [20]. A molecule-molecule reaction is supposed to have a high energy barrier and the four-center reaction producing two IF molecules, with either both in the ground state or one of them in an excited state, is a symmetry forbidden process. The text book mechanism has either I$_2$ or F$_2$ molecules first dissociating into atoms followed by the radical chain reactions F + I$_2 \rightarrow$ IF + I and I + F$_2 \rightarrow$ IF + F. However, neither of these reactions is exothermic enough to produce electronically excited IF.

The clue that something new might be happening in this reaction was actually discovered in a crossed molecular beams study of the F + CH$_3$I $\rightarrow$ IF + CH$_3$ reaction [21]. When we found that this reaction proceeded through the formation of a long lived complex, we began to increase the collision energy to see whether it was possible to shorten the lifetime enough to make it comparable to the rotational period of the CH$_3$IF complex. If we could estimate the lifetime of the collision complex using the rotational period as a clock, it would be possible to evaluate the stability of this reaction intermediate using statistical theories for the unimolecular decomposition rate constants. At higher collision energies, the angular distribution of products monitored at m/e= 146 (IF+) showed a peculiar feature which could not possibly be due to IF produced from the F + CH$_3$I reaction. This was later shown to be from stable CH$_3$IF produced in the collision volume of the two beams which yielded additional IF$^+$ signal after dissociative ionization.

The stable CH$_3$IF was in fact formed by the reaction of undissociated F$_2$ in our F atom beam with CH$_3$I:

$$CH_3I + F_2 \rightarrow CH_3IF + F.$$
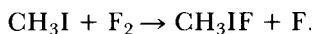
The threshold for this reaction was found to be 11 kcal/mol as shown in Fig. 7. The product angular distribution measured at a collision energy of 25.1 kcal/mol is shown in Fig. 8. Since the dissociation energy of F$_2$ is 37 kcal/mol, the dissociation energy of CH$_3$IF $\rightarrow$ CH$_3$I + F could be as high as 26 kcal/mol (Fig. 9). This was certainly a surprising result and was entirely unsuspected.

In the reaction of I$_2$ and F$_2$, it was not surprising that the stability of the I$_2$F radical is the driving force for the reaction
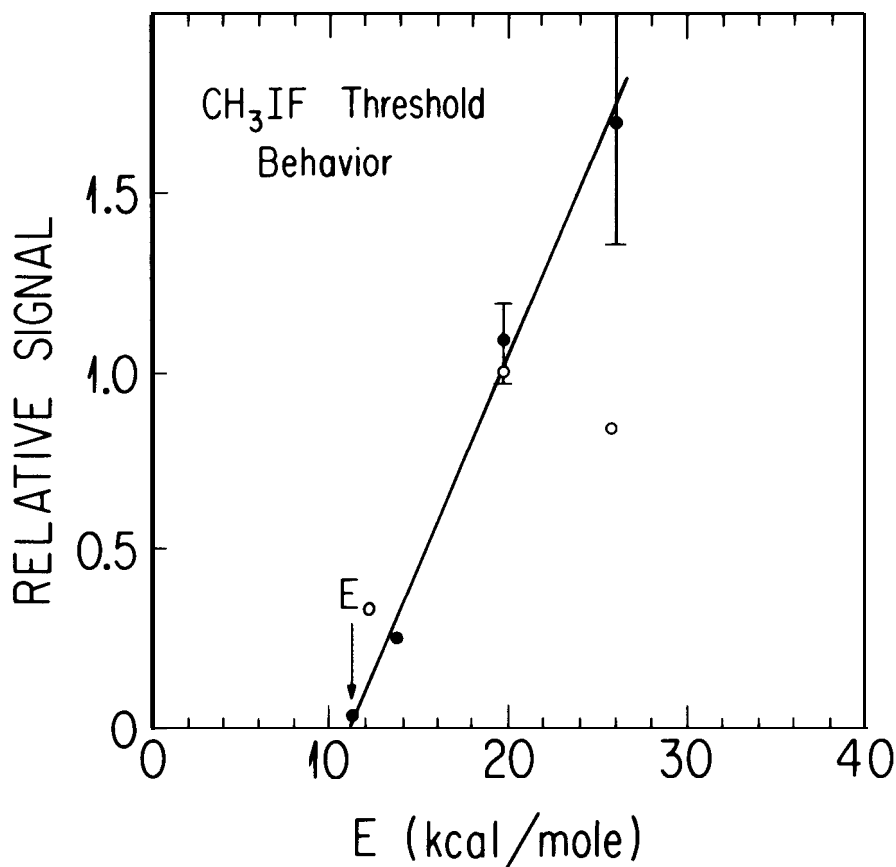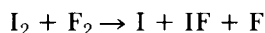
$$I_2 + F_2 \rightarrow I_2F + F$$
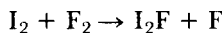
Fig. 7. The kinetic energy dependence of the production of CH_3IF in the $F_2 + CH_3I \rightarrow CH_3IF + F$ reaction.

to proceed. But, what amazed us most was that this reaction had a threshold of only 4 kcal/mol, and that at 7 kcal/mol the reaction

$$I_2 + F_2 \rightarrow I + IF + F$$

was observed [22]. The production of I and IF in this reaction is most likely through the secondary decomposition of vibrationally excited I_2F radicals. Later, a careful investigation showed that the threshold energy for producing electronically excited iodofluoride, IF* [23],

$$I_2 + F_2 \rightarrow IF^* + IF$$
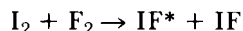
is identical to that for $I_2F + F$ formation. However, the formation of electronically excited IF* is only a minor channel compared to $I_2F + F$ formation. Apparently, it is a secondary encounter between the departing F atom and the terminal I atom in I_2F which produces IF*. A relatively rare sequential process during a binary collision between F_2 and I_2 is responsible for the production of electronically excited IF, not the symmetry forbidden four-center reaction which breaks and forms two bonds simultaneously.
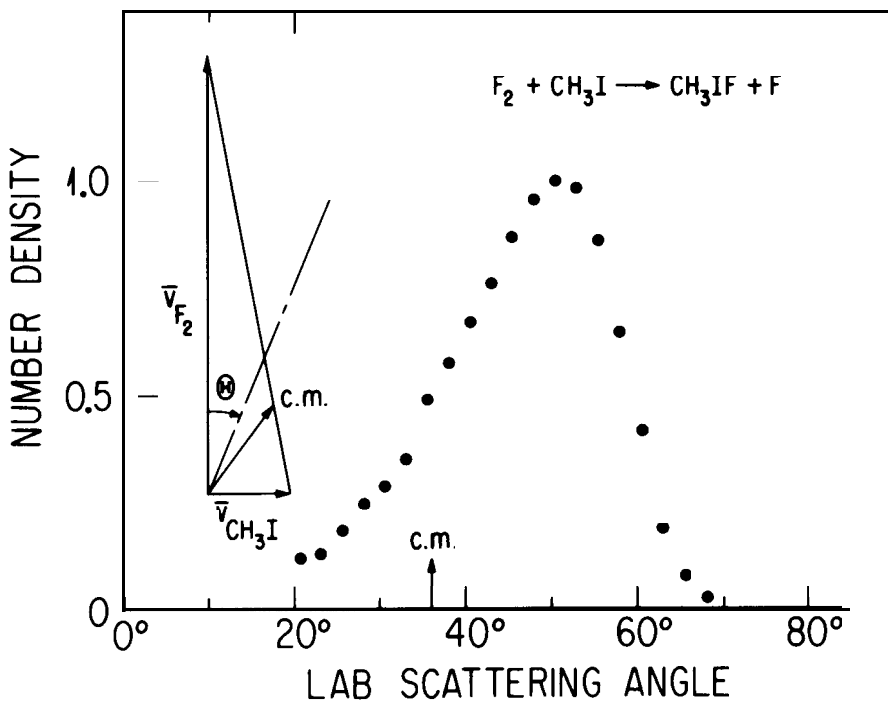
Fig. 8. CH$_3$IF angular distribution, obtained in the reaction of F$_2$+ CH$_3$IF+CH31F + F at a collision energy of 25.1 kcal/mol.
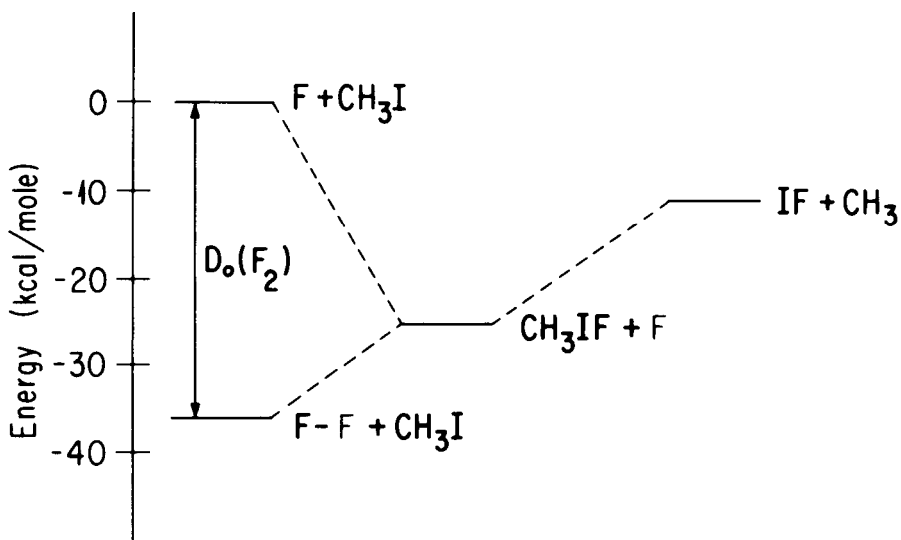

Fig. 9. Energy diagram showing the relative energy CH$_3$IF intermediate in the reaction of F + C H$_3$I $\rightarrow$ CH$_3$+ IF and as a product of the endothermic F$_2$+ CH$_3$I $\rightarrow$ CH$_3$IF + F reaction.
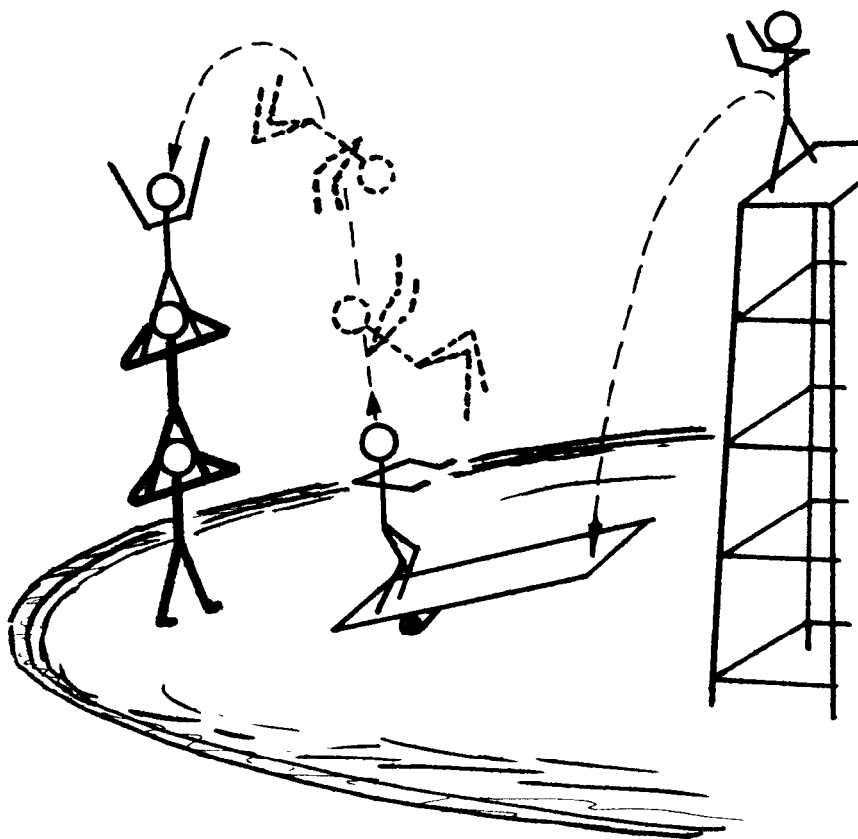
Fig. 10. An acrobat bounced off the plank converts his kinetic energy into potential energy on his way to forming a delicate three-man formation. Many delicate radicals which can not be synthesized through exothermic channels were synthesized by this method.

The fact that one can control kinetic energy precisely and carry out a synthetic study of delicate new radicals through endothermic reactions is certainly among the most dramatic features of crossed molecular beams experiments. Successful studies of the stabilities of a series of I-F containing radicals such as HIF, ClIF and I$_2$F were carried out by transferring the correct amount of kinetic energy into potential energy, just like an acrobatic performance in a circus in which an acrobat is bounced off of a plank and lands gently on the shoulder of a second acrobat who is standing on top of a third to form a fragile three acrobat formation (Fig. 10).

The development of the seeded supersonic beam source has been largely responsible for making crossed molecular beams experiments at higher collision energies possible [24]. If a gaseous mixture is expanded into a vacuum chamber through a small nozzle with a sufficiently high stagnation pressure, all molecules, regardless of their molecular weights, attain the same average terminal speed. Consequently, the kinetic energies of molecules in the beam will be proportional to their molecular weights, and for heavier atoms or
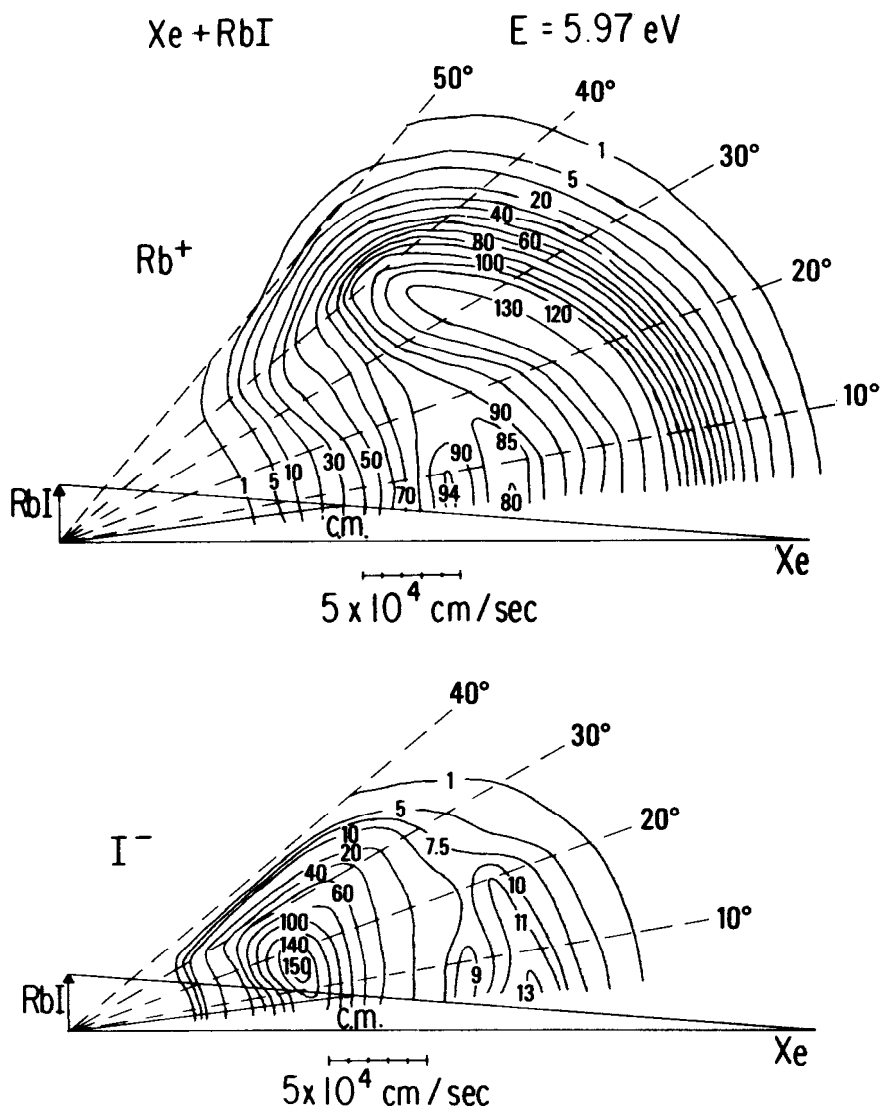
Fig. *11*. Cartesian contour map of Rb⁺ and I⁻ angular and velocity distributions resulting from dissociative Xe + RbI collisions at a most probable relative collision energy of 5.97 eV.

molecules a very high kinetic energy can be obtained by seeding a small fraction of heavy particles in a very light carrier gas.

Using this aerodynamic acceleration for heavier particles many interesting experiments have been carried out in our laboratory. In the collision induced dissociation of alkali halides by rare gas atoms [25], it was found from classical trajectory simulations of velocity and angular distributions of the products that for most dissociative collisions at energies near the dissociation threshold, the most efficient means of transferring translational energy into internal energy is

through initial bond compression in near collinear collisions. The experimental angular and velocity distributions of Rb^+ and I^- from the reaction $Xe + RbI \rightarrow Xe + Rb^+ + I^-$ at a collision energy of 5.97 eV is shown in Fig. 11. The amount of energy transferred as measured from the final translational energy distributions of dissociated atoms agrees with the estimated initial momentum transfer to one of the atoms in the diatomic molecule using the impulse approximation.
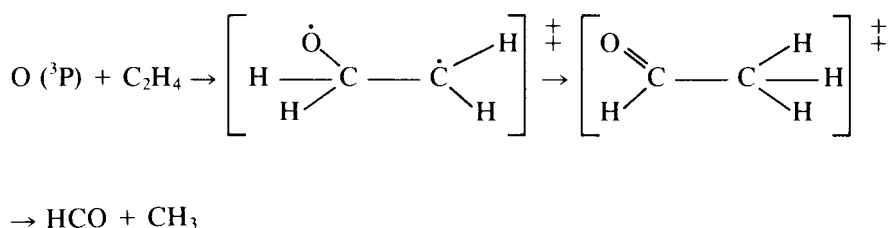
In a recent series of investigations of substantially endothermic reactions of Br atoms eith ortho-, meta- and para-chlorotoluenes, a beam of energetic Br atoms was used to study of reactivity and dynamics of C1 atom substitution by Br atoms [26]. The intermediates of these reactions are expected to have potential wells which are much shallower than the endothermicity of reaction. From the measurements of the translational energy dependence of the reaction cross sections and the product translational energy distributions, the extent of energy randomization among various vibrational degrees of freedom was found to be rather limited. Despite the fact that ortho- and para-chlorotoluenes react easily, no substitution was observed for meta-chlorotoluene indicating that the electron density distribution on the benzene ring strongly influences the reactivity, even though dynamic factors are expected to be more important in endothermic substitution reactions.

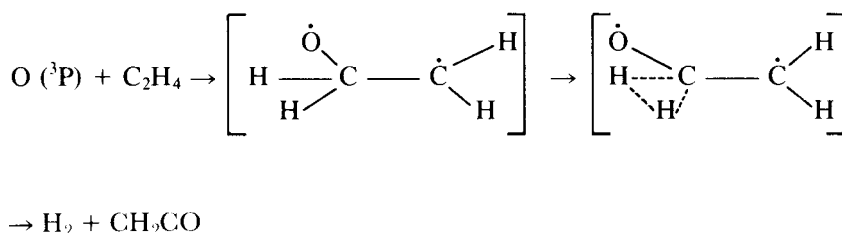*Elucidation of Reaction Mechanisms from Product Angular and Velocity Distributions.*
In elementary chemical reactions involving complicated polyatomic molecules, the unravelling of the reaction mechanism is often the most important issue. Without the positive identification of primary products, it is not possible to discuss reaction dynamics in a meaningful way. In bulk experiments, the identification of primary products has often been complicated by fast secondary reactions of primary products. Recently, advances in sensitive detection methods and time resolved laser techniques have allowed single collision experiments to become possible even in the bulk, and complications caused by secondary collisions can be avoided. However, the positive identification of internally excited polyatomic radicals produced under single collision conditions is still a very difficult problem. Spectroscopic techniques which are so powerful in providing state resolved detection of atoms or diatomic molecules are often not very useful, either because of the lack of spectroscopic information or simply because huge numbers of states are involved. The more general mass spectrometric technique, which depends heavily on "fingerprints" of fragment ions for positive identification, also suffers from the fact that fragmentation patterns for vibrationally excited polyatomic radical products in electron bombardment ionization are not known. This problem is especially serious because many radicals do not yield parent ions. Even if stable molecules are formed as products, the change in fragmentation patterns with increasing internal energy can be so drastic that erroneous conclusions are often reached. For example, at room temperature both ethanol (C_2H_5OH) and acetaldehyde (CH_3CHO) will yield $C_2H_5OH^+$ and CH_3CHO^+ as major ions by electron bombardment ionization. However, since both these ions contain a very weak bond and most

of the vibrational energy is retained in the ionization process, when highly vibrationally excited C_2H_5OH and CH_3CHO are ionized, even if parent ions are initially produced, they will further dissociate into $C_2H_5O^+$ and CH_3CO^+ by ejecting an H atom [27].

   The problem of product identification caused by the fragmentation of primary products during the ionization process can be overcome if product angular and velocity distributions are measured carefully in high resolution crossed molecular beams experiments. For example, the reaction between $=O(^3P)$ and C_2H_4, under single collision conditions using a mass spectrometer to detect the products generates signal at m/e=43,42,29,27, and 15. The fact that m/e= 15 (CH_3^+) and 29 (HCO^+) are the most intense signals suggests that $CH_3 +$ HCO is the major reaction channel. This conclusion is in agreement with previous studies of the reaction of $O(^3P)$ with C_2H_4 carried out by Cvetanovic [28], Pruss et al. [29], and Blumenberg et al. [20]. From the analysis of final products in a bulk experiment using photoionization detection of products with hydrogen Lyman-α (10.2 eV) radiation and electron bombardment ionization mass spectrometry, it was concluded that formation of CH_3 and HCO, resulting from 1,2 migration of a hydrogen atom in the reaction intermediate and subsequent C-C rupture, as shown below, provides 90 percent of the products.

$$O\ (^3P) + C_2H_4 \rightarrow \left[H \overset{\dot{O}}{\underset{H}{\diagup}} C \overline{\quad\quad} \dot{C} \overset{H}{\underset{H}{\diagdown}} \right]^{+\atop+} \rightarrow \left[\overset{O}{\underset{H}{\diagdown}} C \overline{\quad\quad} C \overset{H}{\underset{H}{\diagdown}}H \right]^{+\atop+}$$

$$\rightarrow HCO + CH_3$$

The remaining 10 percent is ketene formed by a three center elimination of an H_2 molecule from the reaction intermediate.

$$O\ (^3P) + C_2H_4 \rightarrow \left[H \overset{\dot{O}}{\underset{H}{\diagup}} C \overline{\quad\quad} \dot{C} \overset{H}{\underset{H}{\diagdown}} \right] \rightarrow \left[\overset{\dot{O}}{H\text{-}\text{-}\text{-}}C \overline{\quad\quad} \dot{C} \overset{H}{\underset{H}{\diagdown}} \right]$$

$$\rightarrow H_2 + CH_2CO$$

   The measurements of product angular distributions in a crossed molecular beams experiment [31], as shown in Fig. 12, gave strong evidence that the above conclusion was not quite correct. The fact that the intense m/e=42 signal and the weak m/e=43 signal (not shown) have the same angular distributions indicates that the substitution reaction forming vinyloxy radical, $CH_2CHO + H$, occurs. The m/e=42 signal ($C_2H_2O^+$) results from dissocia-
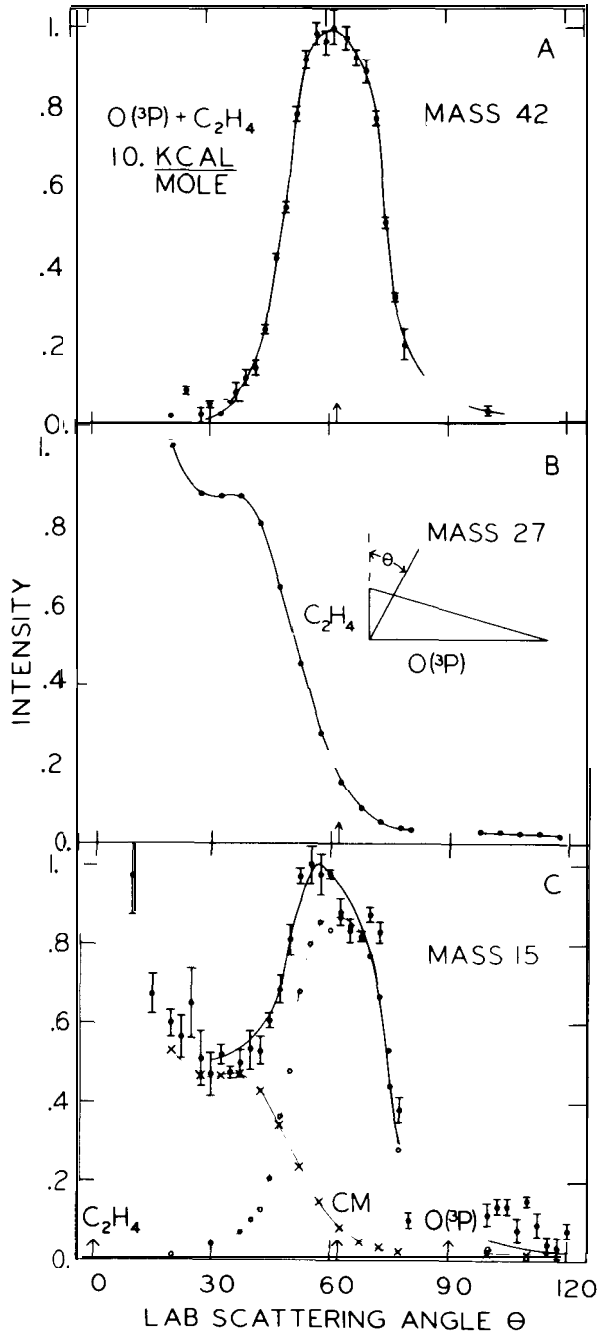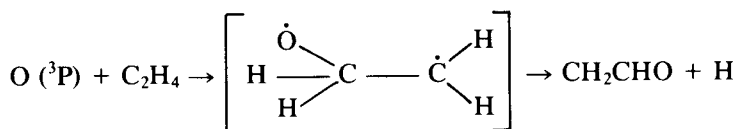
Fig. 12. Angular distributions from the reaction O + C_2H_4 at 10.7 kcal/mol collision energy. (A) CH_2CHO product, (B) elastic scattering of C_2H_4 monitored at m/e=27 ($C_2H_3^+$), (C) m/e=15 (CH_3^+), contributions from C_2H_4 and CH_2CHO are indicated by x and o respectively.

tive ionization of CH$_2$CHO product rather than from the formation of CH$_2$CO and H$_2$. The formation of CH$_2$CO through the three center elimination of a hydrogen molecule is expected to release a larger amount of recoil energy and the fact that CH$_2$CO is recoiling from H$_2$ rather than from an H atom will cause the laboratory angular distribution of CH$_2$CO to be much broader than that of CH$_2$CHO. The m/e= 15 (CH$_3^+$) angular distribution clearly shows that in addition to reaction products, elastically scattered C$_2$H$_4$ molecules also produce CH$_3^+$ ions during ionization. The angular distribution of scattered C$_2$H$_4$ can be unambiguously measured at m/e=27 (C$_2$H$_3^+$). After substracting the contribution from elastically scattered C$_2$H$_4$ from the angular distribution at m/e= 15, it is quite clear that the residual angular distribution of reactively scattered CH$_3^+$ has an identical angular distribution to that measured at m/e 43 and 42. Apparently, most of the CH$_3^+$ from reactive scattering are also daughter ions of vinyloxy radicals, CH$_2$CHO. If the product channel CH$_3$+ HCO were dominant the angular distribution of CH$_3^+$ would be much broader. Without the measurement of product angular or velocity distributions which reveal the parent-daughter relations one would not have suspected that the simple substitution reaction forming vinyloxy radical

$$O\ (^3P) + C_2H_4 \rightarrow \left[H \overset{\dot{O}}{\underset{H}{\longrightarrow}} C \underset{}{\overset{}{\text{———}}} \dot{C} \overset{H}{\underset{H}{\diagdown}} \right] \rightarrow CH_2CHO + H$$

is in fact the major channel.

This was certainly a shocking discovery to chemical kineticists, since the reaction mechanism, $O(^3P) + C_2H_4 \rightarrow CH_3 + HCO$, was thought to be well established. The important role played by the CH$_2$CHO + H channel was never suspected. Several recent bulk studies using various time resolved spectroscopic techniques [32−36] have verified the major role played by the hydrogen subsitution channel indicated by the crossed molecular beams experiments. These were not strictly single collision experiments, but all showed that the reaction channel CH$_2$CHO + H accounted for at least half of the products.

For the reaction of oxygen atoms with benzene the story is quite similar [37]. In earlier mass spectrometric studies of the reaction products under single collision conditions, it was concluded that in addition to the formation of a stable addition product, CO elimination from the reaction intermediate to form C$_5$H$_6$ was another major pathway. The CO elimination mechanism was mostly based on the experimental observation that m/e = 66 and 65 (C$_5$H$_6^+$ and C$_5$H$_5^+$) were the most intense signals. However, the angular distribution of products monitored at m/e = 66 and 65 in the crossed molecular beams experiments clearly show that they are different from each other but very similar to those monitored at m/e = 94 and 93 [C$_6$H$_5$O H$^+$ and C$_6$H$_5$O$^+$], respectively. Apparently, C$_5$H$_5^+$ ions observed are not from neutral C$_5$H$_5$ product, but are actually daughter ions of the phenoxy radical C$_6$H$_5$O. The fact that the very weak signals at m/e = 94 and 93 have different angular distributions, as also

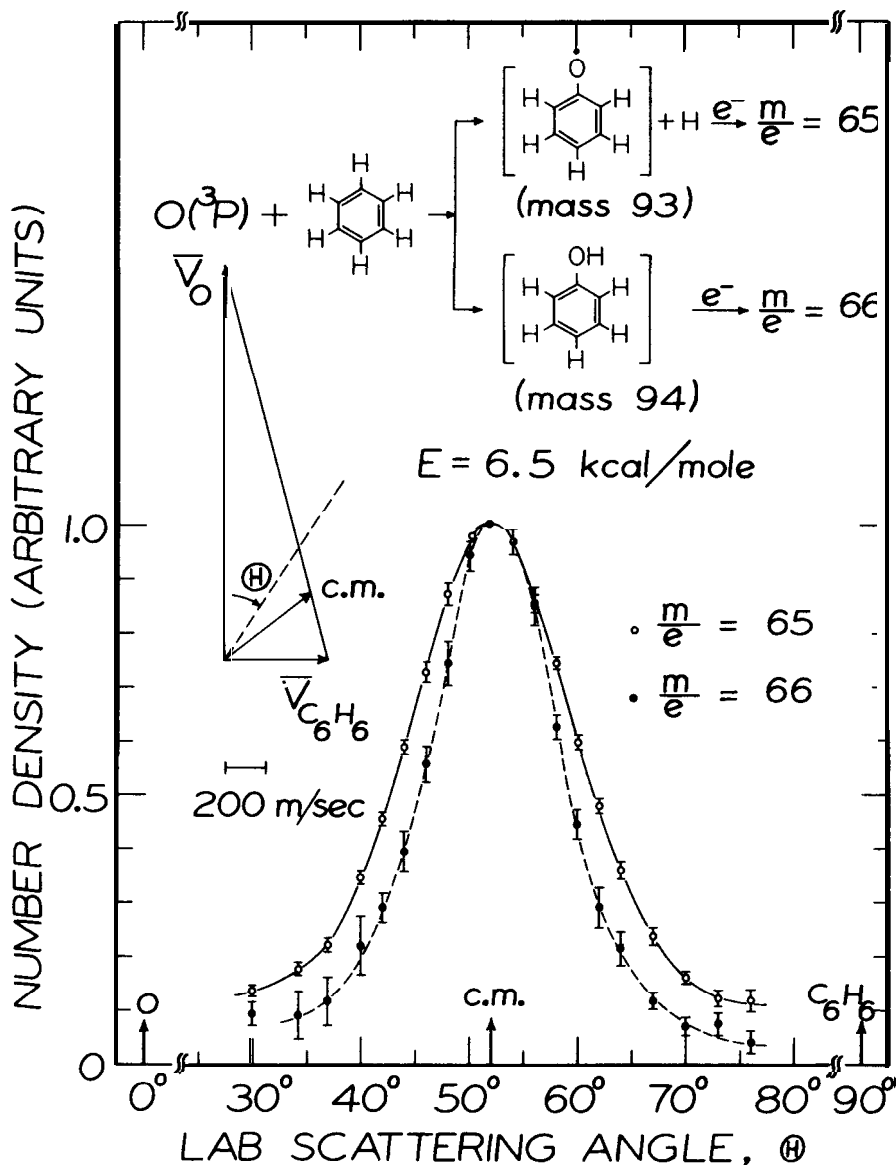Fig. 13. Angular distributions from the reaction $O(^3P)$ + C_6H_6, at a collision energy of 6.5 kcal/mol. The primary reaction products formed were C_6H_5O and C_6H_5OH, which subsequently fragmented during electron bombardment ionization.

reflected in the angular distributions of m/e = 66 and 65 shown in Fig. 13, is convincing evidence that the m/e = 93 signal ($C_6H_5O^+$) is not entirely from the dissociative ionization of the addition product, C_6H_5OH. It is the substitution reaction, in which an oxygen atom replaces a hydrogen atom in the benzene molecule, which causes the angular distribution of the phenoxy product, C_6H_5O, to be broader than that of the adduct, C_6H_5OH. The benzene ring does not seem to open up after the initial attack of an oxygen atom. The

subsequent decomposition of phenoxy radicals appears to be the important ring opening step. Crossed beams studies of substitution reactions of oxygen atoms with a series of halogenated benzenes [38], indeed showed that very highly vibrationally excited phenoxy radicals, produced by substituting bromine and iodine atoms in bromo- and iodobenzene with oxygen atoms, undergo decomposition to eliminate CO.

The fact that each product in a crossed molecular beams experiment has a unique angular and velocity distribution and the requirements that total mass number in a chemical reaction be conserved and that a pair of products from a given channel have the ratio of their center-of-mass recoil velocities inversely proportional to their mass ratio in order to conserve linear momentum are three of the main reasons why measurements of product angular and velocity distributions are so useful in the positive identification of reaction products, even in those cases where none of the products yield parent ions in mass spectrometric detection [9]. In fact, there is no other general method more useful in elucidating complex gas phase reaction mechanisms and providing information on the energetics and dynamics.

Molecular beam studies of photochemical processes
In the investigation of reaction dynamics, lasers have become increasingly important. Not only are they used extensively for the preparation of reagents and quantum state specific detection of products, but they have also become indispensable for the investigation of the dynamics and mechanisms of photo-chemical processes.

One of the more exciting application of lasers in crossed molecular beams experiments is the control of the alignment and orientation of electronically excited orbitals before a reactive encounter. For example, in the reaction of Na with O_2 [39, 40], if lineary polarized dye lasers are used to sequentially excite Na atoms from the 3S to 3P to 4D states, the electronically excited 4D orbital can be aligned along the polarization direction of the electric field vector of the lasers. Consequently, the effect of the alignment of the excited orbital on chemical reactivity can be studied in detail by simply rotating the polarization of the lasers with respect to the relative velocity vector.

For many atom-molecule reactions that proceed directly without forming long-lived complexes, for example, $K + CH_3I$, $F + H_2$ and D_2, and $Na(4D) + O_2$, the dependence of chemical reactivity on the molecular orientation can be obtained from measurements of product angular distributions. For symmetric top moleculars, control of molecular orientation in the laboratory frame is possible, and careful investigations of the orientation dependence of chemical reactivity have been carried out for many systems. The combination of laser induced alignment of excited atomic orbitals and measurements of product angular distributions provide the first opportunity for the detailed experimental probing of the correlation between the alignment of the excited atomic orbital and the orientation of the molecule in a reactive encounter between an atom and a molecule.

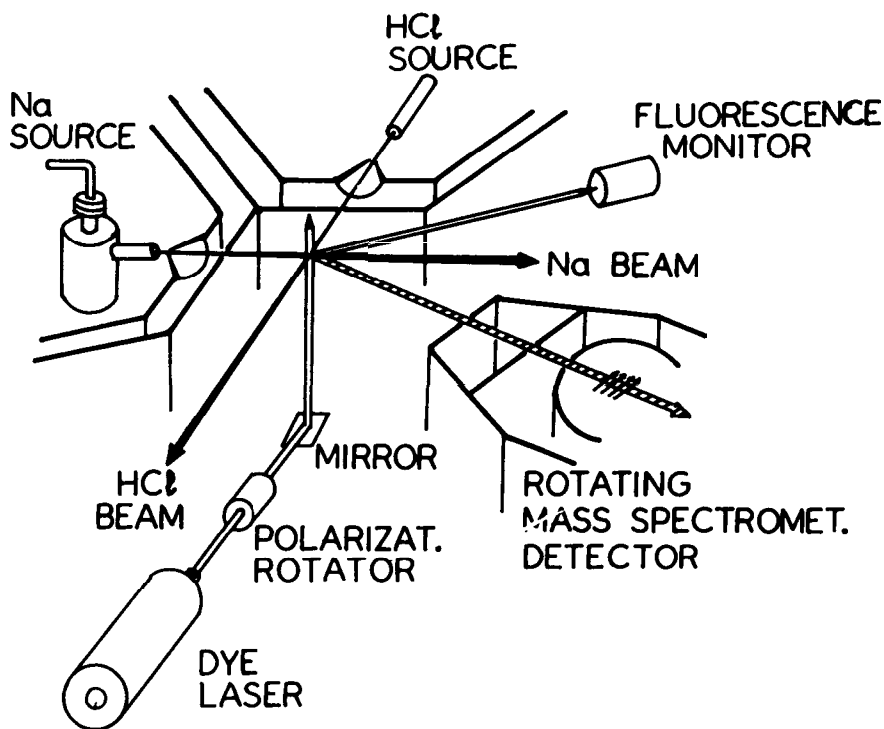The experimental arrangement for the reactive scattering of electronically

Fig. 14. Cut-out view the experimental apparatus for the reactive scattering ofelectronically excited sodium atoms with various molecules.

excited Na with simple molecules is schematically shown in Fig. 14. Because the radiative lifetimes of electronically excited Na are short, excitation and alignment have to be carried out in the intersection region of the two beams.

The reaction of ground state Na atoms with O_2

$$Na(3S) + O_2 \rightarrow NaO + O$$
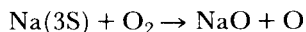
is substantially endothermic. Even if Na is electronically excited to the 3P state, it is still slightly endothermic, and excess translational energy in the reactants was not found to promote NaO formation in our recent experiments. Further excitation of Na from 3P to either the 4D or 5S state, which require comparable excitation energies, makes NaO formation highly exothermic, but only Na(4D) reacts with O_2 and then only at collision energies greater than 18 kcal/mol. The NaO produced is sharply backward peaked with respect to the Na atom beam. As in the low energy reactive scattering of F + $D_2 \rightarrow$ DF + D, the Na(4D) and two O atoms must be lined up collinearly in order for chemical reaction to take place. Such a strict entrance channel configuration with a high threshold energy for Na(4D) + $O_2 \rightarrow$ NaO + O and the lack of chemical reactivity for Na(5S) are quite astonishing for a system in which electron transfer from Na to O_2 is expected to take place at a relatively large separation.
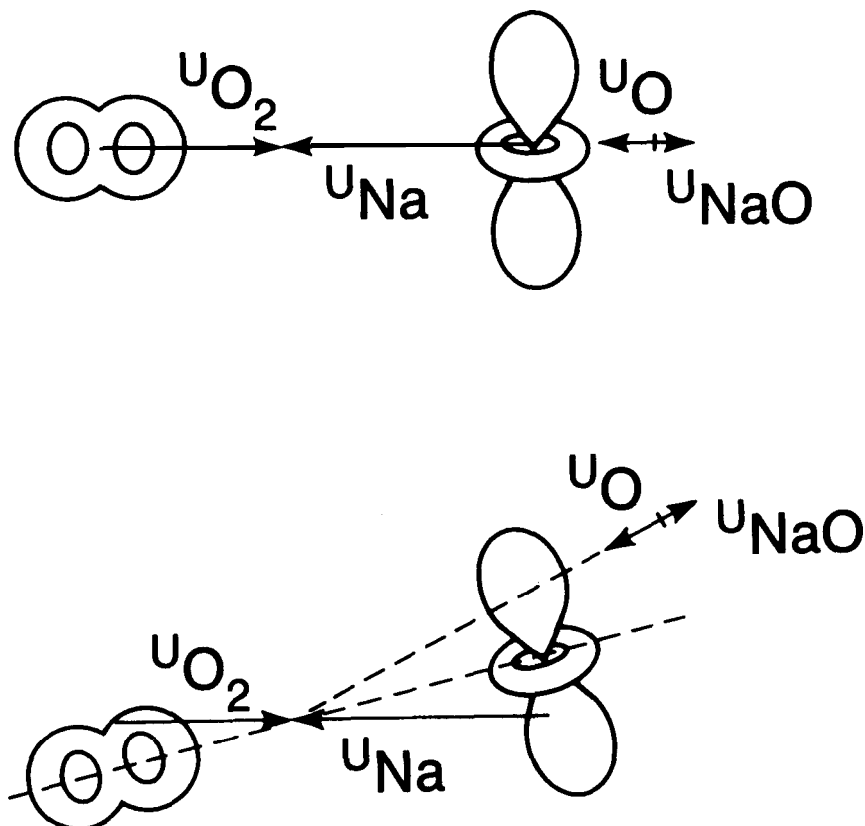
Fig. 1.5. From the measurements of polarization dependence at various angles, the required geometry for reaction was shown to have the Na-O-O intermediate collinear, so that with increasing impact parameter, the Na-O-O axis must be tilted with respect to the relative velocity vector. The Na(4d$_z^2$) orbital remains perpendicular to the Na-O-O axis as shown.

The 4D state of Na prepared by sequential excitation using linearly polarized lasers has an electron density distribution similar to that of the d$_z^2$ orbital in a H atom, if we take the laser polarization axis to be the Z-axis. Rotation of this excited 4D orbital with respect to the relative velocity vector was found to cause a strong variation in reactivity. The reactively scattered signal reaches a maximum when the d$_z^2$ orbital approaches O$_2$ perpendicularly to the relative velocity vector as shown in Fig. 15. The polarization dependence of products appearing at different scattering angles reflects the strong preference for the d$_z^2$ orbital to be aligned perpendicularly to the O$_2$ molecular axis as shown in the bottom frame of Fig. 15.

These experimental observations are contrary to what one would expect from simple theoretical considerations. Because O$_2$ has a finite electron affinity, the Na(4D)-O$_2$ potential energy surface is expected to cross the Na$^+$-O$_2^-$ surface at at relatively large internuclear distance and the long range electron transfer from Na(4D) to O$_2$, to form a Na+O$_2^-$ intermediate, should play an

important role. If this chemically activated $Na^+O_2^-$ complex is indeed responsible for the formation of an ionic NaO product, the reaction should proceed with a large cross section at low collision energies. Also, because the most stable structure of $Na^+O_2^-$ is an isosceles triangle, the angular distribution of NaO product should show either forward peaking or forward-backward symmetry.

Apparently, this long range electron transfer, in spite of its importance, is not the mechanism by which NaO product is formed, and may lead only to the quenching of electronically excited Na(4D) through an inelastic scattering process. It appears that only those collinear collisions that have the d_z2 orbital of Na(4D) aligned perpendicularly to the molecular axis can effectively avoid the long range electron transfer. Then, with this configuration and sufficient collision energy, Na and O_2 could follow a covalent surface to reach a very short Na-O distance where the electron from Na(4D) is transferred to an electronically excited orbital of O_2 after which the complex can separate as Na^+O^- and O.

Na(4D) + $NO_2 \rightarrow$ NaO + NO is a substantially more exothermic reaction, but it has many features which are similar to those found in the Na (4D) + $O_2 \rightarrow$ NaO + O reaction [41]. First of all, the high translational energy requirement, >18 kcal/mol, for NaO product formation again indicates that the entrance channel is very restricted and is likely to be along an O-N bond. If a Na(4D) atom must approach an NO_2 molecule along an O-N bond at a high translational energy in order for a chemical reaction to occur, the orbital angular momentum between Na(4D) and NO_2 will overwhelm the molecular angular momentum of NO_2, coplanar scattering will dominate, and NaO product will be scattered in the plane of the NO_2, which also contains the relative velocity vector. In other words, when Na(4D) approaches NO_2 along the NO bond, all the forces between the interacting atoms will lie in the plane of the NO_2, and the scattered NaO will be confined to that plane. Thus the detector, which rotates in a plane containing both the Na and NO_2 beams, can only detect those NaO products which are produced from NO_2 molecules lying in this plane at the instant when the reactions take place. In contrast to the collinear approach of Na and O_2, there is no cylindrical symmetry about the O-N axis when Na approaches NO_2 along that axis. Because of this, the reaction will depend not only on the d_z^2 orbital alignment in the plane defined by the beams and the detector, but also on the alignment of the d_z^2 about the relative velocity vector. This is exactly what we have observed in the laboratory. The reactivity of Na(4D) + $NO_2 \rightarrow$ NaO + NO as a function of the d_z^2 orbital alignment with respect to the NO_2 molecule is shown in Fig. 16. The most favorable approach has the d_z^2 orbital approaching the O-N axis perpendicularly and lying in the plane of the NO_2. When the alignment of the d_z^2 orbital is rotated in the plane of the NO_2 the reactivity is reduced as the d_z^2 orbital comes closer to being collinear with the O-N axis. When the d_z^2 orbital is rotated out of the NO_2 plane from this collinear configuration, the reactivity decreases further and reaches a minimum when the orbital perpendicular to the NO_2 plane.
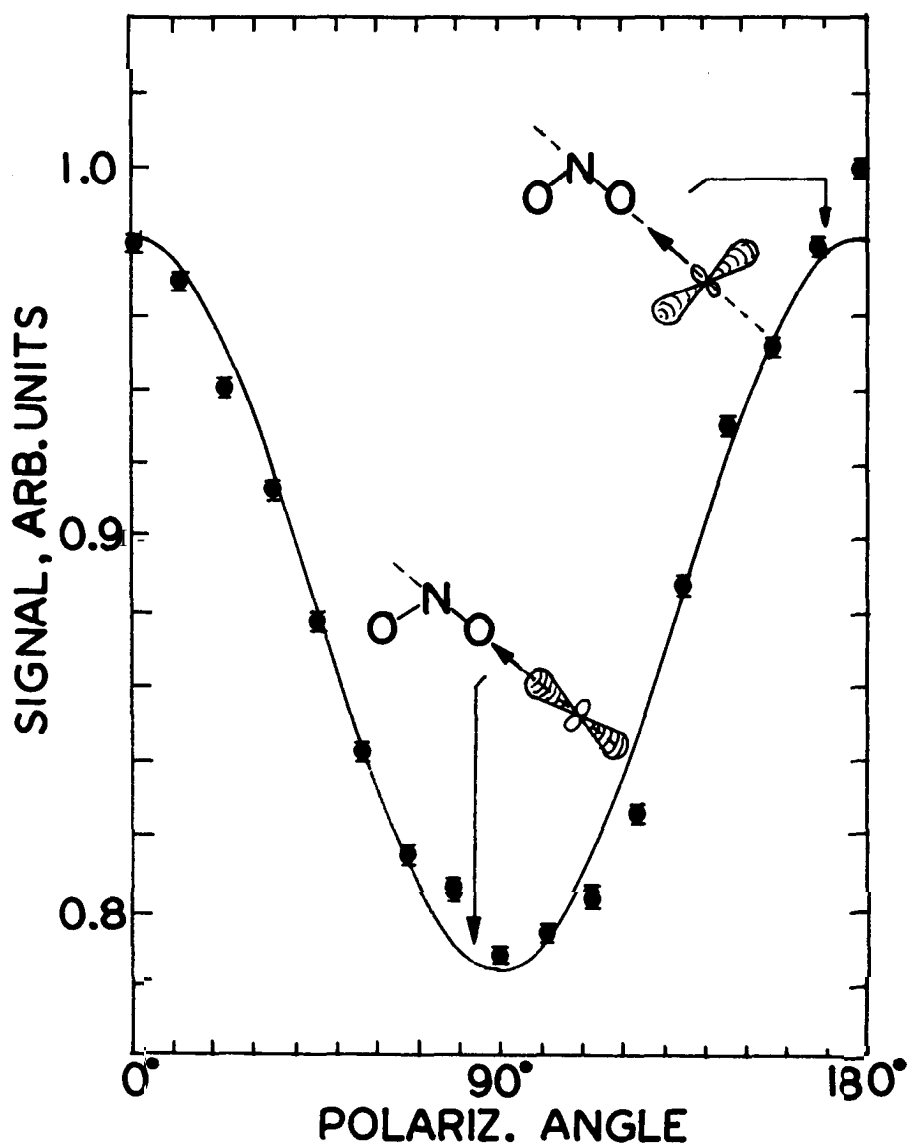
Fig. 16. Polarization dependence of NaO signal from the Na(4D) + NO₂→ NaO + NO reaction. As the (4d$_z$²) orbital of Na was rotated in the plane which contains both beams and the detector, the signal was found to reach a maximum when the (4d$_z$²) orbital was perpendicular to the relative velocity vector and reached a minimum when it was parallel.

The reaction of ground state Na atoms with HCl is endothermic by 5.6 kcal/ mol. Figure 17 shows the product NaCl angular distributions for Na(3S, 3P, 4D) at an average collision energy of 5 kcal/mol. These angular distributions were measured at m/e = 23 because most of the NaCl fragments yield Na⁺in the electron bombardment ionizer. The rising signal at low angles is due to elastically scattered Na atoms. The reactive cross section increases with in-
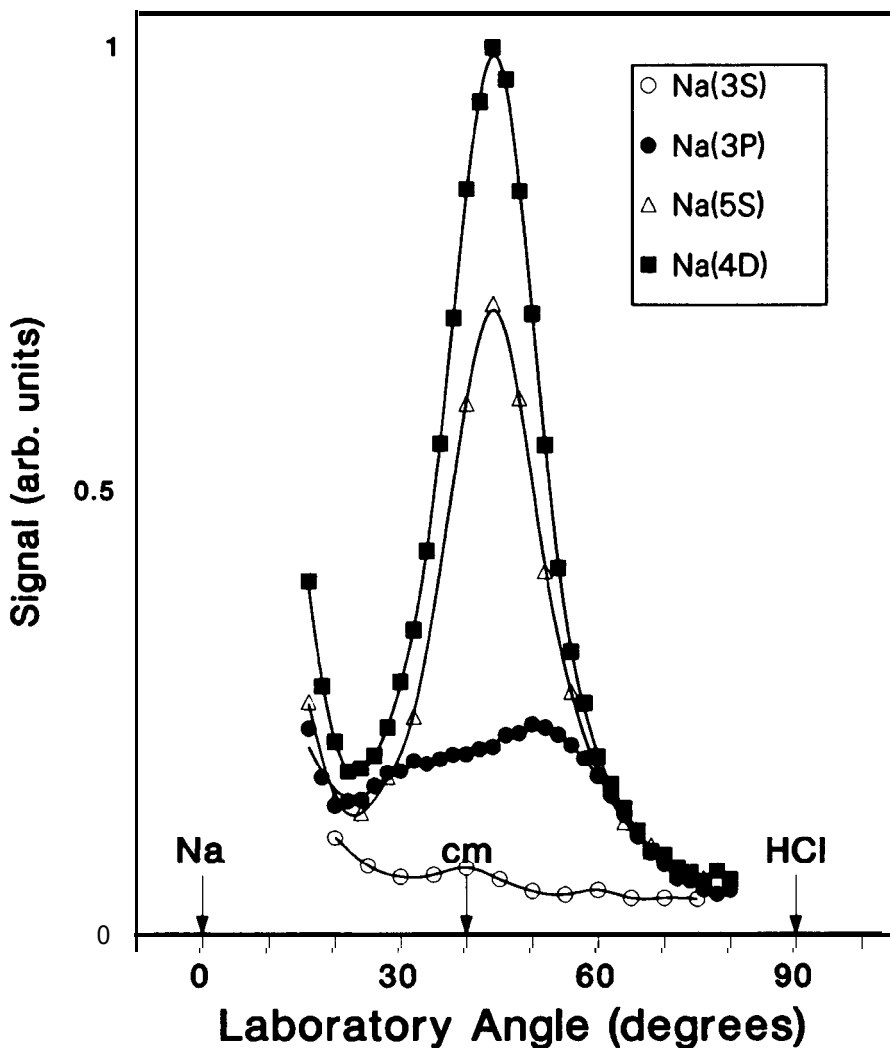
Fig. 17. NaCl angular distributions for Na (3S, 3P, 4D, 5S) + HCl at a collision energy of 5.6 kcal/ mol.

creasing electronic energy. At the collision energy shown, the Na(3S) ground state atoms react because the high velocity components of each beam just barely overcome the endothermicity of the reaction. For the reaction of the Na(3P) atoms, NaCl product is observed over the full laboratory angular range possible allowing for the conservation of the momentum and total energy of the system. This implies a broad range of product translational energies, a conclusion which is supported by product velocity measurements. The same is not true of the reaction of the Na(4D) and Na(5S) states, in which the NaCl is scattered over a narrower angular range than that produced from the Na(3P) state, indicating less translational energy despite an additional 2 eV of excess
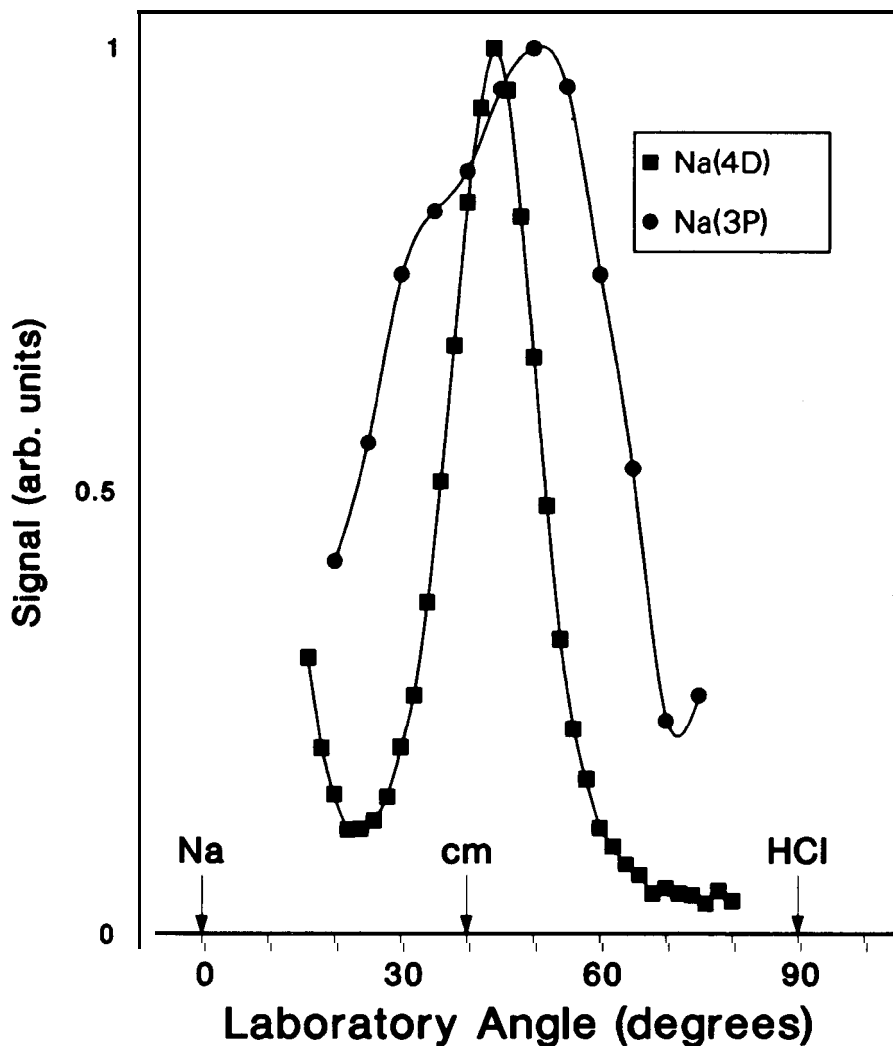
Fig. 18. NaCl angular distributions for Na(3P,4D) + HCl at a collision energy of 5.6 kcal/mol from Fig. 17. The peak intensity of the distribution arising from the reaction of Na(3P) is normalized to that arising from Na(4D) allowing comparison of the angular widths of the two distributions.

energy. This is illustrated in Fig. 18 in which the Na(3P) and Na(4D) angular distributions from Fig. 17 have both been normalized.

These interesting results can be explained by invoking electron transfer followed by repulsion the H atom and NaCl products. HCl is known to be dissociated by slow electrons, and has a *negative* vertical electron affinity of approximately 1 eV. For the reaction of the Na(3P) atoms this electron transfer becomes energetically possible at 3.5 Å. This is, incidentally, the peak of the Na(3P) orbital density. What the departing H atom feels is the repulsion from the Cl atom of the fully developed closed shell NaCl molecule, and a significant

impulse is given to it, In the case of the Na(4D) atoms, the crossing of the neutral and ionic potential curves (the initial point of electron transfer) moves out to 7.7 Å. Thus, an electron transfers over, HCl⁻ dissociates, the H atom departs and the Na⁺ and Cl⁻ are drawn together. The highly vibrationally excited NaCl cannot get rid of any of its energy as the H atom is already gone. The H atom has only felt the repulsion of the loosely bound or highly vibrationally excited NaCl. This interpretation is borne out by the polarization measurements in which the favored alignment of the Na(4D) orbital for reactive signal at any laboratory detector angle is along the relative velocity vector of the system. This corresponds to pointing the 4d orbital towards the HCL, because at long range the relative velocity vector in the laboratory is from the Na to the HCl.

Such a detailed study of the dependence of reactivity on the orbital alignment and the molecular orientation is possible only by combining the crossed molecular beams method with laser excitation.

Concluding remarks

The experimental investigation of elementary chemical reactions is presently in a very exciting period. The advancement in modern microscopic experimental methods, especially crossed molecular beams and laser technology, had made it possible to explore the dynamics and mechanisms of important elementary chemical reactions in great detail. Through the continued accumulation of detailed and reliable knowledge about elementary reactions, we will be in a better position to understand, predict and control many time-dependent macroscopic chemical processes which are important in nature or to human society.

In addition, because of recent improvements in the accuracy of theoretical predictions based on large scale ab initio quantum mechanical calculations, meaningful comparisons between theoretical and experimental findings have become possible. In the remaining years of the twentieth century, there is no doubt that the experimental investigation of the dynamics and mechanisms of elementary chemical reactions will play a very important role in bridging the gap between the basic laws of mechanics and the real world of chemistry.

The experimental investigations described in this article would not have been possible without the dedicated efforts of my brilliant and enthusiastic coworkers during the past twenty years. I enjoyed working with them immensely and sharing the excitement of carrying out research together.

I entered the field of reaction dynamics in 1965 as a post-doctoral fellow in the late Bruce Mahan's group at Berkeley, and learned a lot about the art of designing and assembling a complex experimental apparatus from many scientists and supporting staff at the Lawrence Berkeley Laboratory while studying ion-molecule scattering. In February of 1967, I joined Dudley Herschbach's group at Harvard as a post-doctoral fellow. There, I was exposed to the excitement of the crossed molecular beams research and participated in the construction of an universal crossed molecular beams apparatus. Dudley's contagious enthusiasm and spectacular insight motivated not only me, but a whole generation of chemical dynamicists.
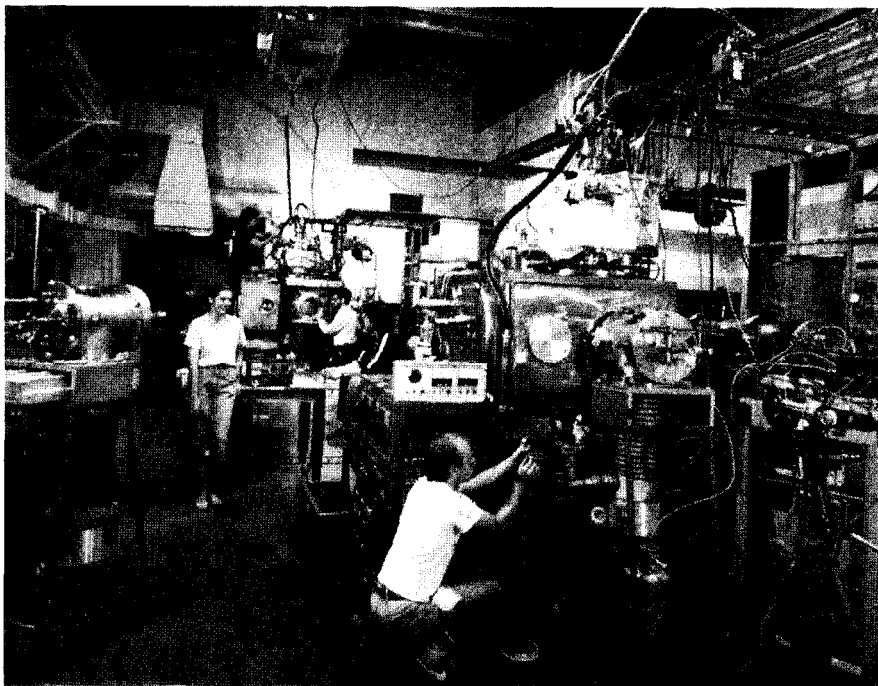
Fig. 19. Part of the new molecular beam laboratory at the University of California, Berkeley.

Molecular collision dynamics has been a wonderful area of research for all practitioners. This is especially true for those who were following the footsteps of pioneers and leaders of the field twenty years ago. In my early years, I was also inspired by the pioneering research work of Sheldon Datz and Ellison Taylor, Richard Bernstein, John Ross, and Ned Green, as well as the "super-sonic" John Fenn. They have been most generous and caring scientists and all of us admire them. Their work is the main reason why the field of molecular beam scattering has attracted many of the best minds in the world and made it a most exciting and rewarding field.

My associations with the University of Chicago (1968-74) and with the University of California, Berkeley (1974-) have been very rewarding. I could not ask for a better environment to pursue an academic career. The stimulating colleagues and excellent facilities as shown in Fig. 19 are what made these institutions so wonderful.

Throughout all these years, my scientific research activities have been supported continuously by the Office of Basic Energy Sciences of the Department of Energy and the Office of Naval Research. The stable and continuing support and the confidence they have shown in my research have been most important and are gratefully appreciated.

REFERENCES

1. H. Eyring and M. Polanyi, Z. Phys. Chem. *B12* (1931) 279.
2. J.C. Polanyi and D.C. Tardy, J. Chem. Phys. *51* (1969) 5717.
3. J.H. Parker and G.C. Pimentel, J. Chem. Phys. *51* (1969) 91.
4. H.W. Cruse, P.J. Dagdigian, and R.N. Zare, Farady Discussion of the Chemical Society, 55 (1973) p. 277.
5. D.P. Gerrity and J.J. Valentini, J. Chem. Phys. 82 (1985) 1323.
6. D.R. Herschbach, in *Les Prix Nobel* 1986, Nobel Foundation, 1987.
7. R.B. Bernstein, *Chemical Dynamics via Molecular Beam and Laser Techniques,* Oxford University Press, 1982.
8. D.M. Neumark, A.M. Wodtke, G.N. Robinson, C.C. Hayden, K. Shobatake, R.K. Sparks, T.P. Schaefer, and Y.T. Lee, J. Chem. Phys. 82 (1985) 3067.
9. Y.T. Lee, in *Atomic and Molecular Beam Method,* edited by G. Scoles and U. Buck, Oxford University Press, 1986.
10. Y.T. Lee, J.D. McDonald, P.R. LeBreton and D.R. Herschbach, Rev. Sci. Instr. 40 (1969) 1402.
11. J.T. Muckerman, in *Theoretical Chemistry-Advances and Perspectives,* edited by H. Eyring and D. Henderson (Academic Press, New York, 1981), Vol. 6A, l-77.
12. C.F. Bender, P.K. Pearson, S.V. O'Neill, and H.F. Schaefer, J. Chem. Phys. 56 (1972) 4626; Science, 176 (1972) 1412.
13. D.G. Truhlar and A. Kuppermann, J. Chem. Phys. *52* (1970) 384; 56 (1972) 2232.
14. S.F. Wu and R.D. Levine, Mol. Phys. 22 (1971) 991.
15. G.C. Schatz, J.M. Bowman, and A. Kuppermann, J. Chem. Phys. 63 (1975) 674.
16. A. Kuppermann, in *Potential Energy, Surfaces and Dynamics Calculations,* edited by D.G. Truhlar (Penum Publishing Corporation, New York, 1981).
17. J.M. Launay and M. LeDourneuf, J. Chem. Phys. *B15* (1982) L455.
18. R.E. Wyatt, J.F. McNutt, and M.J. Redmon, Ber. Bunsenges. Chem. Phys. 86 (1982) 437.
19. D.M. Neumark, A.M. Wodtke, G.N. Robinson, C.C. Hayden, and Y. T. Lee, J. Chem. Phys. 82 (1985) 3045.
20. J.W. Birks, S.D. Gabelnick, and H.S. Johnston, J. Mol. Spectr. 57 (1975) 23.
21. J.M. Farrar, and Y.T. Lee, J. Chem. Phys. 63 (1975) 3639.
22. M.J. Coggiola, J.J. Valentini, and Y.T. Lee, Int. J. Chem. Kin. 8 (1976) 605.
23. C.C. Kahler and Y.T. Lee, J. Chem. Phys. 73 (1980) 5122.
24. N. Abuaf, J.B. Anderson, R.P. Andres, J.B. Fenn, and D.R. Miller *Rarefied Gas Dynamics,* Fifth Symposium 1317-1336 (1967).
25. F.P. Tully, N.H. Cheung, H. Haberland, and Y.T. Lee, J. Chem. Phys. 73 (1980) *4460.*
26. G.N. Robinson, R.E. Continetti, and Y.T. Lee, to be published Faraday Disc. Chem. Soc. 84 (1987).
27. F. Huisken, Krajnovich, Z. Zhang, Y.R. Shen, and Y.T. Lee, J. Chem. Phys. 78 *3806* (1983).
28. R.J. Cvetanovic, Can. J. Chem. 33 (1955) 1684.
29. F.J. Pruss, J.R. Slagle, and D. Gutman, J. Phys. Chem. 78 (1974) 663.
30. B. Blumenberg, K. Hoyerman and R. Sievert, Proc. 16th Int. Symp. on Combution, The Combustion Institute, 1977, p. 841.
31. R.J. Buss, R.J. Baseman, G. He, and Y.T. Lee, J. Photochem. *17* (1981) 389.
32. G. Inoue and H. Akimoto, J. Chem. Phys. 74 (1981) 425.
33. H.E. Hunziker, H. Kneppe, and H.R. Wendt, J. Photochem. 17 (1981) 377.
34. F. Temps and H.G. Wagner, Max Planck Inst. Stromungsforsch. Ber. 18 (1982).
35. U.C. Sridharan and F. Kaufman, Chem. Phys. Lett. *102* (1983) 45.
36. Y. Endo, S. Tsuchiya, C. Yamada, and E. Hirota, J. Chem. Phys. 85, (1986) 4446.
37. S.J. Sibener, R.J. Buss, P. Casavecchia, T. Hirooka, and Y.T. Lee, J. Chem. Phys. 72 (1980) 4341.

38. R.J. Brudzynski, A.M. Schmoltner, P. Chu, and Y.T. Lee, to be published in J. Chem. Phys. 1987.
39. H. Schmidt, P.S. Weiss, J.M. Mestdagh, M.H. Covinsky, and Y. T. Lee Chem. Phys. Lett. *118* (1985) 539.
40. P.S. Weiss PH.D. Thesis, University of California, 1986.
41. B.A. Balko, H. Schmidt, C.P. Schulz, M.H. Covinsky, J.M. Mestdagh, and Y.T. Lee, to be published Faraday Disc. Chem. Soc. 84 (1987).